



NTNU – Trondheim
Norwegian University of
Science and Technology

Dynamic two phase flow models for flushing

Ahmadreza Rahbari

Master of Science in Mechanical Engineering

Submission date: June 2014

Supervisor: Ole Jørgen Nydal, EPT

Co-supervisor: Zhilin Yang, EPT

Norwegian University of Science and Technology
Department of Energy and Process Engineering

EPT-M-2014-92

MASTER THESIS

for

Student Ahmadreza Rahbari

Spring 2014

Dynamic two phase flow models for flushing*Dynamiske tofase strømningsmodeller for fortrenkning i rørstrøm***Background and objective**

Dynamic flow models are in widespread use for a large variety of oil-gas flow simulations. Two basic schemes are applied: a mixture formulation with a slip relation and a two fluid formulation. The two methods shall be compared for the case of flushing of one liquid by another. The mixture formulation often assumes a relative velocity (slip) due to steady flows. A question is then on the comparisons of the schemes for transient flows: how fast can the flushing rates be before the two formulations depart and acceleration effects become significant.

Matlab scripts are available as basis for the work (non-iterative and implicit time integration). A C++ program is also available, including both a two fluid and a mixture formulation.

The following tasks are to be considered:

- 1 A short review of the equations for two fluid and mixture models, with applications for flushing simulations with separated flows
- 2 Implement numerical solver for drift flux and for two fluid model, for separated flows
- 3 Test for available oil-water flushing cases from the laboratory, comparing drift flux (steady state slip relation) and two fluid models
- 4 Conclusions and recommendations

Within 14 days of receiving the written text on the master thesis, the candidate shall submit a research plan for his project to the department.

When the thesis is evaluated, emphasis is put on processing of the results, and that they are presented in tabular and/or graphic form in a clear manner, and that they are analyzed carefully.

The thesis should be formulated as a research report with summary both in English and Norwegian, conclusion, literature references, table of contents etc. During the preparation of the text, the candidate should make an effort to produce a well-structured and easily readable report. In order to ease the evaluation of the thesis, it is important that the cross-references are correct. In the making of the report, strong emphasis should be placed on both a thorough discussion of the results and an orderly presentation.

The candidate is requested to initiate and keep close contact with his/her academic supervisor(s) throughout the working period. The candidate must follow the rules and regulations of NTNU as well as passive directions given by the Department of Energy and Process Engineering.

Risk assessment of the candidate's work shall be carried out according to the department's procedures. The risk assessment must be documented and included as part of the final report. Events related to the candidate's work adversely affecting the health, safety or security, must be documented and included as part of the final report. If the documentation on risk assessment represents a large number of pages, the full version is to be submitted electronically to the supervisor and an excerpt is included in the report.

Pursuant to "Regulations concerning the supplementary provisions to the technology study program/Master of Science" at NTNU §20, the Department reserves the permission to utilize all the results and data for teaching and research purposes as well as in future publications.


The final report is to be submitted digitally in DAIM. An executive summary of the thesis including title, student's name, supervisor's name, year, department name, and NTNU's logo and name, shall be submitted to the department as a separate pdf file. Based on an agreement with the supervisor, the final report and other material and documents may be given to the supervisor in digital format.

- Work to be done in lab (Multiphase Flow Lab)
 Field work

Department of Energy and Process Engineering, 14. January 2014



Olav Bolland
Department Head


Ole Jorgen Nydal
Academic Supervisor

Research Advisor: Zhilin Yang

Preface

This thesis is submitted to the Norwegian University of Science and Technology (NTNU) as a part of the 5-year's master's program.

This work has been carried out at the Department of Energy and Process Engineering. It has been a privilege to take on this challenging project under supervision of Professor Ole Jørgen Nydal. I would like to thank Professor Nydal for his support in this work. Moreover, I would like to thank Ivar Eskerud Smith and Milad Khatibi from Department of Energy and Process Engineering, and especially Sissel Jensen Nefzaoui who became my mentor since I came to Norway.

In the end, I would also like to thank my parents, Firouzeh and Alireza, for their support throughout my education.

Abstract

This thesis aims at modeling the separated liquid-liquid flows with application for flushing. In the beginning, there will be a short review of the governing equations and the fundamental concepts used in this thesis. Two models are introduced and developed based on the two PhD dissertations [15] and [11]. The properties of the fluids in these models are based on Oil, Exxsol D80, $\mu_o = 1.79[cP]$ and tapped water, $\mu_w = 1.11[cP]$. These models will be numerically developed for both dynamic and stationary flows. The numerical scheme used for these models is explicit. A complete explanation about discretization is given in chapter 4.

After developing the dynamic and stationary solutions for both models, there will be two major case studies. The first one is to understand when the dynamic and stationary solutions depart from one another as the mixture velocity varies between low velocities to high velocities. It turns out that The solutions look quite similar until the mixture velocity reaches the value of around $U_M = 1[m/s]$. Then the solutions become more and more different especially at the oil front.

The second case study is about keeping the mixture velocity constant and varying the pipe angle. The pipe angle variation range lies between -2.5° and $+5^\circ$. For negative inclinations, the dynamic and stationary solutions agree quite well. However when the positive slope is put to the test and gravity is acting against the flow, the dynamic and stationary solutions differ more. Finally there will be a discussion on where this different behavior stems from. The two fluid model introduced at the beginning of this report is studied closely, term by term. These terms represent the frictional forces that balance the pressure gradient in the pipe. These forces are plotted for four different cases with mixture velocities varying from $U_M = 0.25[m/s]$ to $U_M = 5[m/s]$. These figures reveal which forces dominate the solution for relatively low and high mixture velocities. The dominating forces are the ones that balance the pressure gradient. It turns out that the level gradient is quite significant and a dominant term in almost all cases. However as the mixture velocity increases, the acceleration terms grow to the same order of magnitude as the level gradient. But for the most part, the spatial and the temporal acceleration act symmetrically, and in effect cancel each other out. There will be a thorough discussion about this in the final chapter.

Nomenclature

Abbreviations

USO	Superficial velocity of oil
USW	Superficial velocity of water

Symbols

α_o	Oil holdup	$[-]$
α_w	Water holdup	$[-]$
β	Reverse density	$[\frac{kg}{m^3}]$
ϵ	Wall roughness	$[-]$
\hat{n}	Normal vector	$[-]$
μ_k	Dynamic viscosity phase k	$[Pa.s]$
ρ_m	Mixture density	$[\frac{kg}{m^3}]$
ρ_o	Oil density	$[\frac{kg}{m^3}]$
ρ_w	Water density	$[\frac{kg}{m^3}]$
τ_i	Shear stress at the oil-water interface	$[\frac{N}{m^2}]$
τ_{Wo}	Wall shear stress on the oil side	$[\frac{N}{m^2}]$
τ_{Ww}	Wall shear stress on the water side	$[\frac{N}{m^2}]$
φ	Pipe inclination	$[rad]$
A	Pipe's cross sectional area	$[m^2]$
D	Diameter	$[m]$
$D_{h,k}$	Hydraulic diameter phase k	$[m]$
f_i	Wall friction factor at the oil-water interface	$[-]$
f_o	Wall friction factor on the oil side	$[-]$
f_w	Wall friction factor on the water side	$[-]$
g	Gravitational acceleration	$[\frac{m}{s^2}]$
h	Line fraction	$[-]$
p	Pressure	$[\frac{N}{m^2}]$
Re_k	Reynolds number phase k	$[-]$

S	Perimeter	$[m]$
t	time	$[s]$
u_m	Mixture velocity	$[\frac{m}{s}]$
u_o	Oil phase velocity	$[\frac{m}{s}]$
u_s	Slip velocity oil/water	$[\frac{m}{s}]$
u_w	Water phase velocity	$[\frac{m}{s}]$
V	Momentum slip	$[\frac{N.s}{m^3}]$
x	Spatial coordinate	$[m]$

Contents

Preface	I
Abstract	II
Nomenclature	III
1 Introduction	1
1.1 Background	1
1.1.1 Liquid-liquid flows	1
1.2 Literature review	2
1.2.1 Dynamic simulation and CFD models	3
1.3 Objectives	3
1.4 Fundamental Definitions	3
2 Incompressible Two-Phase Flow Models	5
2.1 Model I	5
2.2 Model II	8
2.3 Closure Models	10
3 Summary of The Two-Fluid Incompressible Models	11
3.1 Model I	11
3.1.1 Solution Strategy	11
3.2 Model II	12
3.2.1 Solution Strategy	12
4 Discretization and numerical solution	13
4.1 general numerical solution	13
4.1.1 Grid	13
4.1.2 Discretization	13
4.1.3 Boundary condition	14
4.2 Discretizing model I	14
4.3 Model I-steady state discretization	16
4.4 Discretizing model II	16
4.5 Model II-steady state discretization	17
5 Validating the model and sensitivity analysis	18
5.1 Sensitivity analysis on mixture velocity for horizontal pipes	18
5.1.1 Model I	18
5.1.2 Model II	22
5.2 Sensitivity analysis on pipe angle	25
5.2.1 Model I	25
5.2.2 Model II	29
5.3 Model Limitations	33
5.4 Grid sensitivity in space and time	33

6 Discussion	36
6.1 Comparison the magnitude of the terms in the momentum equations for oil and water	36
6.1.1 Case I: $U_M = 0.25$	37
6.1.2 Case II: $U_M = 0.5$	39
6.1.3 Case III: $U_M = 1$	41
6.1.4 Case IV: $U_M = 5$	43
7 Conclusion	45
Appendix A Model I Matlab code	46
Appendix B Model II Matlab code	50
Appendix C Closure models, friction Matlab code	54
References	55

1 Introduction

Multiphase flow is everywhere in petroleum industry. From reservoir, transport through pipelines or tankers all the way to the refineries and to the final products. The better we understand the nature of these flows, the easier it is to develop accurate prediction models for designing and operating such systems. This study aims at developing dynamic and stationary simulation models using separated oil-water flows with application for flushing in horizontal and near horizontal pipes. Before diving into the details of this work, there will be a brief introduction to the liquid-liquid flow subject, literature study followed by a short introduction to the fundamentals concepts and definitions.

1.1 Background

Understanding the fundamentals of multiphase flow dynamics and its properties is essential to design and operation of the multiphase transport pipelines, for both offshore and onshore applications. Studying multiphase flow patterns is a rather new subject compared to the classical fluid mechanics. The systematic research efforts did not appear until around 1950 [12]. Since 1950, the experiments have been conducted in order to understand the complex nature of the multiphase flows. The produced data is used both to validate the existing models or to develop new models or correlations. Since of the studies have been conducted on gas-liquid flows, the amount of experimental data on the two-phase oil-water is rather limited. The existing literature on oil-water flow takes on flow regime changes, pressure drop and hold-up measurements. Most of the studies use the averaged properties and the phases are treated as bulk flows. The detailed flow properties such as velocity profiles are neglected. These studies make the basis for the different correlations used mostly as closure models in addition to the conservation laws in CFD simulations. The averaging of the properties however reduces the accuracy of the models. It is understood that reliable data is a crucial element for a successful prediction model of such flows. Oil-water flows are in a way more complex compared to the gas-liquid flows. This is due to lower density and viscosity ratios, which makes a more complex interfacial behavior between the phases. It is then generally harder to predict flow characteristics such as pressure gradient and slip. For instance, it is observed that for higher water hold-up values are observed for upwardly inclined pipes. In downwardly inclined pipes, lower water hold-up values are observed compared to the horizontal and upwardly inclined pipes [12]

1.1.1 Liquid-liquid flows

Oil-water flows have various flow patterns due to their complex rheological behavior. It is then more challenging to predict the accurate pressure drop or holdup values according to each flow pattern. For the mixed flow liquid regime, this problem can get even more complex since emulsions can form.






<u>DESCRIPTION</u>	<u>SKETCH</u>
<u>STRATIFIED (S):</u> POSSIBLY WITH SOME MIXING AT THE INTERFACE	
<u>MIXED (MO, MW):</u> WITH SEPARATED LAYERS OF A DISPERSION AND "FREE" PHASE	
<u>ANNULAR (AO, AW):</u> CORE OF ONE PHASE WITHIN THE OTHER PHASE	
<u>INTERMITTENT (IO, IW):</u> PHASES ALTERNATELY OCCUPYING THE PIPE AS A FREE PHASE OR AS A DISPERSION	
<u>DISPERSED (DO, DW):</u> HOMOGENEOUS MIXTURE	

Figure 1: Classification of oil water flow patterns, from [2]

Another challenging phenomenon with respect to modeling is the phase inversion, which happens when the dispersed phase switches to the continuous phase. Phase inversion leads to considerable pressure gradient change, for instance from oil-in-water flow to water-in-oil flow. There have been some published results indicating that the oil-water mixture viscosity could increase dramatically at this inversion point, It is highly recommended that the operator should avoid operating an oil-water pipeline at these flow conditions [2].

1.2 Literature review

More research has been carried out on the two-phase oil-gas flows than oil-water flows, and due to the different nature of the liquid-liquid flows, the research results are not directly transferable. One reason is the density difference is considerably smaller for oil-water flow, which causes smaller buoyancy force and a different interfacial dynamics. The flow regime classification has always been subjective according to each researcher. Different techniques and methods have been used in literature to determine the flow patterns and their transition boundaries. Oil-water flows can be generally classified into four main categories

Stratified Flow: Simultaneous flow of two immiscible separate layers. Two continuous phases need to be present in stratified flow.

Dispersed Flow: One phase flow is continuous while the other phase is dispersed in form of droplets or bubbles in the continuous medium.

Annular Flow: One phase forms a film around the pipe with a certain thickness while the other

phase flows at the center of the pipe.

Plug Flow: plugs or oil bubbles follow one another above the water phase in the pipe.

1.2.1 Dynamic simulation and CFD models

When developing CFD models for multiphase flows, the conservation of mass and momentum are solved together with other closure models. Considering the mass balance for each phase, one mass equation is solved for each phase. To solve the mass equations, the superficial velocity and the slip is needed. We can find these variables by solving mass and momentum conservation simultaneously. Wall and interfacial friction models are used to close the system of equations. The relative velocity between the phases is strongly dependent on the flow regime. In stratified flow with phases highly separated from one another, the relative velocity is high while the dispersed flow results in low relative velocities between the phases.

Another way to solve for the relative velocity in oil-water flows is based on pressure gradient and mixture density [9] The simulation of dynamic one-dimensional multiphase pipe flows in the oil and gas industry began around 1980 [10] parallel to the rising need of predicting flow properties. This has led to the birth of OLGA (developed by IFE), the market leader among all commercial simulators until now [10]. LEDA, another emerging commercial package that has been developed by SINTEF, has been commercially available since 2010. Another applicable area for multiphase flow simulations is the nuclear industry, two-phase steam-water. Many codes exist for simulating these flows, including RAMONA, RELAP and TRAC. These are available through the software package TRACE [11]. Several of these codes have been used as an inspiration through developing the multiphase flow codes for the oil and gas industry. However, most nuclear safety codes are based on the schemes explicit in time, while the oil and gas codes are based on the implicit schemes, because the nuclear systems are much faster [11].

There exist as well transient one-dimensional codes based on the drift-flux model. TACITE [14], and TrafFlow by Shell. TrafFlow is now replaced by COMPAS which uses the mixture momentum equation of oil, gas and water. The same approach is taken for the energy equation, and the mass equations for each phase are separately solved. FlowManager pipe simulation is the other program which uses the drift flux model (one single momentum equation) together with the slip models to get the relative velocities between each phases [11]

1.3 Objectives

Develop numerical models for liquid-liquid flows with application for flushing. Compare and analyze the behavior of dynamic and stationary models for different cases of oil-water flushing in horizontal and near horizontal pipes.

1.4 Fundamental Definitions

This section aims at defining the fundamental concepts or properties fundamental to liquid-liquid flows. The following concepts are applied in deriving and explaining the dynamic models. Liquid area fraction: liquid (oil or water) area fraction in the pipe cross section

$$\alpha_k = \frac{A_k}{A} \quad (1.1)$$

The subscript k represents each phase which in this case can be either water or oil. The volumetric flow of each phase and the volumetric water fraction are

$$Q_k \left[\frac{m^3}{s} \right] \quad (1.2)$$

$$WC = \frac{Q_w}{Q_o + Q_w} \quad (1.3)$$

In oil-water applications, the volumetric water fraction is known as the water-cut. Superficial velocity of the phase k is defined as the volumetric flow of the phase divided by the pipe cross section area. This velocity corresponds to the single phase flow velocity of the phase k in the pipe.

$$U_{sk} = \frac{Q_k}{A} \quad (1.4)$$

Having defined the superficial velocity, the volumetric water fraction or the water-cut can be re-written in terms of the superficial velocities.

$$WC = \frac{U_{sw}}{U_{so} + U_{sw}} \quad (1.5)$$

The actual phase velocity is the volumetric flow rate of the phase k per phase area. This definition gives the in-situ velocity of the phase. The value of phase velocity is different than the superficial velocity since the volumetric flow rate of the phase is passing through a smaller area than the pipe's cross section.

$$u_k = \frac{U_{sk}}{\alpha_k} \quad (1.6)$$

The mixture velocity is the sum of the superficial velocities and represents the total volumetric flux.

$$u_m = \sum U_{sk} \quad (1.7)$$

The geometrical relations in stratified flows are reviewed here. They come in handy in calculating the hydraulic diameter of each phase, and shear stress calculations. According to the figure 2:

$$S_1 = D(\pi - \theta) \quad (1.8)$$

$$S_2 = D\theta \quad (1.9)$$

$$S_i = D \sin \theta \quad (1.10)$$

$$h_2 = \frac{D}{2} (1 - \cos \theta) \quad (1.11)$$

$$\pi\alpha_2 = \theta - 0.5 \sin 2\theta \quad (1.12)$$

Where θ is called the half angle, and the above formulation is an implicit expression. Biberg has proposed an explicit approximation where the half angle can be calculated directly from

$$\theta = \pi\alpha_2 + \left(\frac{3\pi}{2} \right)^{1/3} \left(1 - 2\alpha_2 + \alpha_2^{1/3} - \alpha_1^{1/3} \right) \quad (1.13)$$

Geometry of the stratified flow with smooth interface

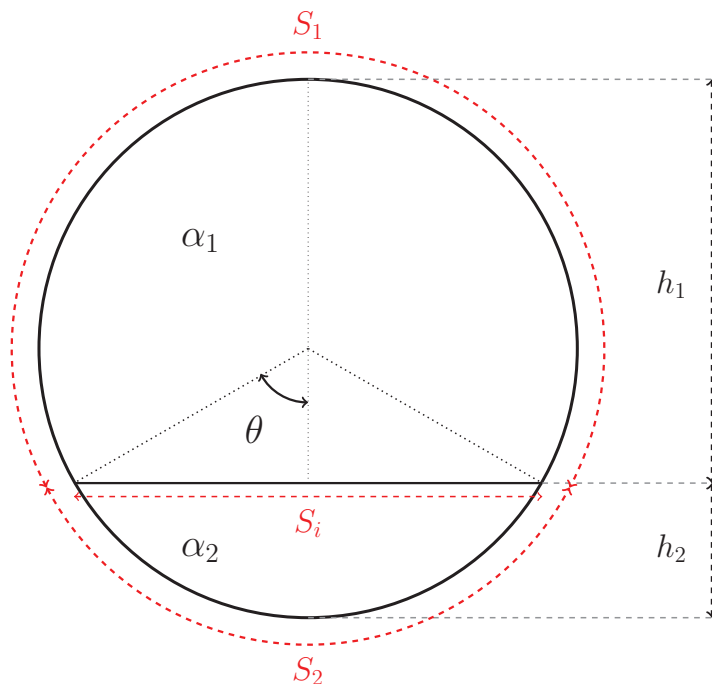


Figure 2: Geometry of the stratified flow

When calculating the Reynolds number in a single phase flow, the pipe diameter is used as a characteristic length. However for stratified flow, a hydraulic diameter is the characteristic length. In case of a stratified oil-gas flow, the gas flow is normally considered as a closed channel, and the oil as open channel flow. The same approach is taken for the oil-water flow here.

$$D_{h1} = \frac{4A\alpha_1}{S_1 + S_2} \quad (1.14)$$

$$D_{h2} = \frac{4A\alpha_2}{S_1} \quad (1.15)$$

2 Incompressible Two-Phase Flow Models

The models developed for CFD programming in this work are based on the PHD dissertations [15] (Model I) and [11] (Model II). The unknown variables in these models are different, however in principle, similar results are expected. The results provided in the following sections, prove this point.

2.1 Model I

The model based on [15], takes the incompressible two fluid model, and after eliminating the pressure drop, reduces the model to a two parameter problem. This has done by introducing two variables β and V and implementing them in the combined momentum equation. β is

called the reverse density and V is the momentum slip. If we have these two variables, along with a constant mixture velocity, we can solve the two-fluid model. In this chapter, the model has been derived and explained. We start by writing the mass conservation equations for two incompressible liquids, namely oil and water.

$$\frac{\partial}{\partial t}(\rho_o \alpha_o) + \frac{\partial}{\partial x}(\rho_o \alpha_o u_o) = 0 \quad (2.1)$$

$$\frac{\partial}{\partial t}(\rho_w \alpha_w) + \frac{\partial}{\partial x}(\rho_w \alpha_w u_w) = 0 \quad (2.2)$$

Since the densities are constant for incompressible fluids, we can cross them out from the equations (2.1) and (2.2) and then come at two volume conservation equations

$$\frac{\partial}{\partial t}(\alpha_o) + \frac{\partial}{\partial x}(\alpha_o u_o) = 0 \quad (2.3)$$

$$\frac{\partial}{\partial t}(\alpha_w) + \frac{\partial}{\partial x}(\alpha_w u_w) = 0 \quad (2.4)$$

When we combine the equations (2.3) and (2.4), the temporal derivative drops out because sum of the volume fractions always equals unity.

$$\frac{\partial}{\partial x}(\alpha_o u_o + \alpha_w u_w) = 0 \quad (2.5)$$

We get the mixture velocity by integrating this equation

$$\alpha_o u_o + \alpha_w u_w = u_m(t) \quad (2.6)$$

Considering constant mixture velocity will be the basis of the simulation and solving of the models. This adds one closure equation (an algebraic equation) to the system of equations we are trying to solve.

$$\frac{\partial}{\partial t}(\rho_o \alpha_o u_o) + \frac{\partial}{\partial x}(\rho_o \alpha_o u_o^2) + \alpha_o \frac{\partial p}{\partial x} + \rho_o \alpha_o g \cos \varphi \frac{\partial h_w}{\partial x} = q_1 \quad (2.7)$$

$$\frac{\partial}{\partial t}(\rho_w \alpha_w u_w) + \frac{\partial}{\partial x}(\rho_w \alpha_w u_w^2) + \alpha_w \frac{\partial p}{\partial x} + \rho_w \alpha_w g \cos \varphi \frac{\partial h_w}{\partial x} = q_2 \quad (2.8)$$

The right hand side of the momentum equations are the friction and gravity terms

$$q_1 = -\frac{\tau_{W_o} S_o}{A} - \tau_i \frac{S_i}{A} - \rho_o \alpha_o g \sin \varphi \quad (2.9)$$

$$q_2 = -\frac{\tau_{W_w} S_w}{A} + \tau_i \frac{S_i}{A} - \rho_w \alpha_w g \sin \varphi \quad (2.10)$$

Taking out the phase fractions from time and space derivatives, and dividing both sides by phase fractions, we get

$$\frac{\partial}{\partial t}(\rho_o u_o) + \frac{\partial}{\partial x}(\frac{1}{2} \rho_o u_o^2) + \frac{\partial p}{\partial x} + \rho_o g \cos \varphi \frac{\partial h_w}{\partial x} = \frac{q_1}{\alpha_o} \quad (2.11)$$

$$\frac{\partial}{\partial t}(\rho_w u_w) + \frac{\partial}{\partial x}(\frac{1}{2} \rho_w u_w^2) + \frac{\partial p}{\partial x} + \rho_w g \cos \varphi \frac{\partial h_w}{\partial x} = \frac{q_2}{\alpha_w} \quad (2.12)$$

Then the pressure drop is eliminated by combining equations (2.11) and (2.12).

$$\frac{\partial}{\partial t}(\rho_o u_o - \rho_w u_w) + \frac{\partial}{\partial x}(\frac{\rho_o u_o^2 - \rho_w u_w^2}{2}) + (\rho_o - \rho_w) g \cos \varphi h_w = \frac{q_o}{\alpha_o} - \frac{q_w}{\alpha_w} \quad (2.13)$$

The unknown variables of the flow are the velocities u_1 and u_2 and the volume fractions α_1 and α_2 . We can solve the two-phase model equations by knowing the slip and one of the phase fractions. Keyfitz introduced two new variables to rewrite the conservation equations [15]. Reverse density:

$$\beta = \rho_w \alpha_o + \rho_o \alpha_w \quad (2.14)$$

Momentum slip

$$V = \rho_o u_o - \rho_w u_w - (\rho_o - \rho_w) u_m \quad (2.15)$$

Now we can rewrite the velocities and volume fractions in terms of reverse density and momentum slip

$$u_o = u_m + \frac{V}{\beta} \alpha_w \quad (2.16)$$

$$u_w = u_m - \frac{V}{\beta} \alpha_o \quad (2.17)$$

$$\alpha_o = \frac{\beta - \rho_o}{\rho_w - \rho_o} \quad (2.18)$$

$$\alpha_w = \frac{\beta - \rho_w}{\rho_o - \rho_w} \quad (2.19)$$

$$\frac{V}{\beta} = u_o - u_w \quad (2.20)$$

Substituting these variables into the mass conservation equations, we get the conservation of reverse density, and substitution of the above variables into the momentum equations gives the final slip model. Combining the two volume conservation equations (2.3) and (2.4) we get

$$\frac{\partial}{\partial t} (\rho_w \alpha_o + \rho_o \alpha_w) + \frac{\partial}{\partial x} (\rho_w \alpha_o u_o + \rho_o \alpha_w u_w) = 0 \quad (2.21)$$

Rewriting the above equation in terms of β and V , the conservation of reverse density becomes

$$\frac{\partial \beta}{\partial t} + \frac{\partial}{\partial x} \left(\frac{V}{\beta} \frac{(\beta - \rho_o)(\beta - \rho_w)}{(\rho_o - \rho_w)} + u_m \beta \right) = 0 \quad (2.22)$$

By substituting the phase velocities from equations (2.16) and (2.17) into the momentum slip balance (2.13), we get the final slip model

$$\frac{\partial V}{\partial t} + \frac{\partial}{\partial x} \left(\frac{V^2}{\beta^2} \frac{\beta^2 - \rho_o \rho_w}{2(\rho_o - \rho_w)} + u_m V + (\rho_o - \rho_w) g \cos \varphi h_w(\beta) \right) = q_v \quad (2.23)$$

The right hand side of the above equation is the source

$$q_v = \frac{q_1}{\alpha_o} - \frac{q_2}{\alpha_w} = \frac{\tau_{W_o} S_o}{\alpha_o A} + \frac{\tau_{W_w} S_w}{\alpha_w A} - \frac{\tau_i S_i}{\alpha_o \alpha_w A} - (\rho_o - \rho_w) g \sin \varphi \quad (2.24)$$

The final slip velocity is solved once including the spatial and temporal derivatives on the left hand side of the equation.

$$\underbrace{\frac{\partial V}{\partial t}}_{Temporal} + \underbrace{\frac{\partial}{\partial x} \left(\frac{V^2}{\beta^2} \frac{\beta^2 - \rho_o \rho_w}{2(\rho_o - \rho_w)} + u_m + (\rho_o - \rho_w) g \cos \varphi h_w(\beta) \right)}_{Spatial} = q_v \quad (2.25)$$

Equation (2.24) is also solved at steady-state conditions by setting the temporal and spatial derivatives equal to zero which gives the algebraic momentum slip equation

$$q_v = \frac{\tau_{W_o} S_o}{\alpha_o A} + \frac{\tau_{W_w} S_w}{\alpha_w A} - \frac{\tau_i S_i}{\alpha_o \alpha_w A} - (\rho_o - \rho_w) g \sin \varphi = 0 \quad (2.26)$$

2.2 Model II

This model is partially based on [11], because we are only studying the liquid-liquid flows without the presence of the gas phase. The model uses the mixture mass balance and a mixture momentum equation. The pressure gradient is also eliminated from the equations, and we are left with two unknown variables in this case are u_s and ρ_m . Considering a constant mixture velocity and solving for these two variables, we can solve the two-fluid model.

$$\rho_m = \alpha_w \rho_w + \alpha_o \rho_o \quad (2.27)$$

$$u_m = \alpha_w u_w + \alpha_o u_o \quad (2.28)$$

$$u_s = u_o - u_w \quad (2.29)$$

The volume fractions and the phase velocity can be written as a function of u_s and ρ_m .

$$\alpha_o = \frac{\rho_w - \rho_m}{\rho_w - \rho_o} \quad (2.30)$$

$$\alpha_w = \frac{\rho_m - \rho_o}{\rho_w - \rho_o} \quad (2.31)$$

$$u_o = u_m + \alpha_w u_s \quad (2.32)$$

$$u_w = u_m - \alpha_o u_s \quad (2.33)$$

To get a mixture mass conservation, we combine equations (2.1) and (2.2)

$$\frac{\partial(\alpha_w \rho_w + \alpha_o \rho_o)}{\partial t} + \frac{\partial(\alpha_w \rho_w u_w + \alpha_o \rho_o u_o)}{\partial x} = 0 \quad (2.34)$$

Rewriting the velocities in terms of the slip velocity and taking into account the above definitions, we get

$$\frac{\partial \rho_m}{\partial t} + \frac{\partial}{\partial x} \left(\alpha_w \rho_w (u_m - \alpha_o u_s) + \alpha_o \rho_o (u_m + \alpha_w u_s) \right) = 0 \quad (2.35)$$

$$\frac{\partial \rho_m}{\partial t} + \frac{\partial}{\partial x} \left(\rho_m u_m - (\rho_w - \rho_o) \alpha_o \alpha_w u_s \right) = 0 \quad (2.36)$$

The volume fractions are functions of mixture velocity according to equations (2.30) and (2.31). Similarly, the momentum equations for oil and water are combined in order to eliminate the pressure gradient term and get the momentum slip equation, which is the second equation of the model.

$$\frac{\partial(\rho_o \alpha_o u_o)}{\partial t} + \frac{\partial(\rho_o \alpha_o u_o^2)}{\partial x} = -\alpha_o \frac{\partial p}{\partial x} - \alpha_o \rho_o g \frac{\partial h_w}{\partial x} \cos \beta - \alpha_o \rho_o g \sin \beta - \frac{\tau_{W_o} S_o}{A} - \frac{\tau_i S_i}{A} \quad (2.37)$$

$$\frac{\partial(\rho_w \alpha_w u_w)}{\partial t} + \frac{\partial(\rho_w \alpha_w u_w^2)}{\partial x} = -\alpha_w \frac{\partial p}{\partial x} - \alpha_w \rho_w g \frac{\partial h_w}{\partial x} \cos \beta - \alpha_w \rho_w g \sin \beta - \frac{\tau_{W_w} S_w}{A} + \frac{\tau_i S_i}{A} \quad (2.38)$$

We can re-write the acceleration terms in the momentum equations to take out the void fractions from the temporal and spatial derivatives in the following steps

$$\begin{aligned} \frac{\partial(\rho_o \alpha_o u_o)}{\partial t} + \frac{\partial(\rho_o \alpha_o u_o^2)}{\partial x} &= u_o \frac{\partial(\rho_o \alpha_o)}{\partial t} + \rho_o \alpha_o \frac{\partial u_o}{\partial t} + u_o \frac{\partial(\rho_o \alpha_o u_o)}{\partial x} + \rho_o \alpha_o u_o \frac{\partial u_o}{\partial x} = \\ &= \underbrace{\left(\frac{\partial(\rho_o \alpha_o)}{\partial t} + \frac{\partial(\rho_o \alpha_o u_o)}{\partial x} \right)}_{=0 \text{ (continuity)}} u_o + \rho_o \alpha_o \frac{\partial u_o}{\partial t} + \rho_o \alpha_o u_o \frac{\partial u_o}{\partial x} = \alpha_o \left(\frac{\partial \rho_o u_o}{\partial t} + \frac{\partial \frac{\rho_o u_o^2}{2}}{\partial x} \right) \end{aligned} \quad (2.39)$$

The same procedure applies to the water momentum equation. We substitute the new acceleration terms and divide the momentum equations (2.37) and (2.38) by the void fractions, we get

$$\frac{\partial \rho_o u_o}{\partial t} + \frac{\partial \frac{\rho_o u_o^2}{2}}{\partial x} = -\frac{\partial p}{\partial x} - \rho_o g \frac{\partial h_w}{\partial x} \cos \beta - \rho_o g \sin \beta - \frac{\tau_{W_o} S_o}{\alpha_o A} - \frac{\tau_i S_i}{\alpha_o A} \quad (2.40)$$

$$\frac{\partial \rho_w u_w}{\partial t} + \frac{\partial \frac{\rho_w u_w^2}{2}}{\partial x} = -\frac{\partial p}{\partial x} - \rho_w g \frac{\partial h_w}{\partial x} \cos \beta - \rho_w g \sin \beta - \frac{\tau_{W_w} S_w}{\alpha_w A} + \frac{\tau_i S_i}{\alpha_w A} \quad (2.41)$$

We eliminate the pressure gradient to get the momentum slip model including the transient terms

$$\begin{aligned} \frac{\partial(\rho_w u_w - \rho_o u_o)}{\partial t} + \frac{\partial \frac{1}{2}(\rho_w u_w^2 - \rho_o u_o^2)}{\partial x} = \\ -(\rho_w - \rho_o)g \frac{\partial h_w}{\partial x} \cos \beta - (\rho_w - \rho_o)g \sin \beta + \frac{\tau_{W_o} S_o}{\alpha_o A} - \frac{\tau_{W_w} S_w}{\alpha_w A} + \frac{\tau_i S_i}{\alpha_o \alpha_w A} \end{aligned} \quad (2.42)$$

We would like to have a system of equations with two unknowns, namely the slip velocity u_s and the mixture density ρ_m . So we write the phase velocities as functions of the mixture and slip velocities as we derived in equations (2.32) and (2.33). We start by manipulating the temporal derivative in the slip momentum

$$\begin{aligned} \frac{\partial}{\partial t}(\rho_w u_w - \rho_o u_o) &= \frac{\partial}{\partial t}((\rho_w - \rho_o) u_m - (\alpha_o \rho_w + \alpha_w \rho_o) u_s) \\ &= \frac{\partial}{\partial t}(\rho_m - (\rho_w + \rho_o)) u_s \end{aligned} \quad (2.43)$$

The time derivative of the term $(\rho_w - \rho_o)u_m$ is zero, because the mixture velocity is considered constant in each case, and the densities are constant as well. The same procedure for the spatial derivative

$$\begin{aligned} \frac{\partial}{\partial x} \frac{1}{2}(\rho_w u_w^2 - \rho_o u_o^2) &= \frac{\partial}{\partial x} \frac{1}{2}(\rho_w (u_m - \alpha_o u_s)^2 - \rho_o (u_m + \alpha_w u_s)^2) \\ &= \frac{\partial}{\partial x} \left((\rho_w - \rho_o) \frac{u_m^2}{2} + (\rho_w \alpha_o^2 - \rho_o \alpha_w^2) \frac{u_s^2}{2} - (\rho_w \alpha_o + \rho_o \alpha_w) u_s u_m \right) \\ &= \frac{\partial}{\partial x} \left((\rho_w \alpha_o^2 - \rho_o \alpha_w^2) \frac{u_s^2}{2} - (\rho_w \alpha_o + \rho_o \alpha_w) u_s u_m \right) \end{aligned} \quad (2.44)$$

The convective term $(\rho_w - \rho_o) \frac{u_m^2}{2}$ is constant with respect to x , so its derivative is zero. If we put the expressions from equations (2.43) and (2.44) back into the momentum slip equation (2.42), we get

$$\begin{aligned} \frac{\partial}{\partial t}(\rho_m - (\rho_w + \rho_o)) u_s + \frac{\partial}{\partial x} \left((\rho_w \alpha_o^2 - \rho_o \alpha_w^2) \frac{u_s^2}{2} - (\rho_w \alpha_o + \rho_o \alpha_w) u_s u_m + (\rho_w - \rho_o) g h_w \cos \beta \right) \\ = \frac{\tau_{W_o} S_o}{\alpha_o A} - \frac{\tau_{W_w} S_w}{\alpha_w A} + \frac{\tau_i S_i}{\alpha_o \alpha_w A} - (\rho_w - \rho_o) g \sin \beta \end{aligned} \quad (2.45)$$

Where the shear stress at the interface is calculated as a function of slip velocity and oil friction factor

$$\frac{\tau_i S_i}{\alpha_o \alpha_w A} = \frac{f_{ow} \rho_o S_i}{8 \alpha_o \alpha_w A} u_s^2 \quad (2.46)$$

If we eliminate the temporal and spatial derivatives, we get the relative velocity u_s from the famous holdup equation.

$$u_s^2 = \frac{8 \alpha_o \alpha_w A}{\rho_o f_{ow} S_i} \left[(\rho_w - \rho_o) g \frac{\partial h_w}{\partial x} \cos \beta + (\rho_w - \rho_o) g \sin \beta - \frac{\tau_{W_o} S_o}{\alpha_o A} + \frac{\tau_{W_w} S_w}{\alpha_w A} \right] \quad (2.47)$$

2.3 Closure Models

Closure models regarding the friction factors apply to both models. Therefore, they are presented here in one section. Wall and interface friction factors in the shear stress terms need to be determined in order to close and solve the system of equations. The shear stress terms at the wall and the interface are:

$$\tau_{W_o} = \frac{1}{8} \rho_o f_o |u_o| u_o \quad (2.48)$$

$$\tau_{W_w} = \frac{1}{8} \rho_w f_w |u_w| u_w \quad (2.49)$$

$$\tau_i = \frac{1}{8} \rho_o f_i |u_o - u_w| (u_o - u_w) \quad (2.50)$$

Where f_k is the friction factor of the phase k and f_i is the shear stress at the interface. Different correlations have been proposed for friction factors. For laminar flows, the wall friction is approximated as:

$$f_{k,laminar} = \frac{64}{Re_k} \quad (2.51)$$

The constant 64 for laminar flows is analytically obtained for flows in pipes with circular cross sections. In stratified flow geometries, especially heavy oil simulations, laminar flow plays an important role. However, the cross section of the oil phase is no longer circular. This might be a source of significant error for such flows [11]. For fully turbulent flows, we use the Haaland's correlation, which is an explicit estimation of the Colbrook's formula

$$\frac{1}{\sqrt{f_{k,turbulent}}} = -1.8 \log\left(\frac{6.9}{Re_k} + \left(\frac{\varepsilon}{3.7D}\right)^{1.11}\right) \quad (2.52)$$

To have a smooth and continuous transition between from laminar to turbulent flow, the friction factor for each phase is implemented in the codes similar the pseudo-code below:

$$\begin{aligned} &\text{if } Re_k < 300 \rightarrow f_k = f_{k,laminar} \\ &\text{else } f_k = \max(f_{k,laminar}, f_{k,turbulent}) \end{aligned}$$

This way, we have determined the oil and water friction factors. Russel has shown that if we assume flat interface, the friction factor at the interface becomes

$$f_i = f_o \quad (2.53)$$

The Reynolds number

$$Re_k = \frac{\rho_k u_k D_{h,k}}{\mu_k} \quad (2.54)$$

Where D_h, k is the hydraulic diameter for each liquid phase. For stratified oil-water flow, the oil phase is modeled as closed channel and the water phase as open channel.

$$D_{ho} = \frac{4A\alpha_o}{S_o + S_i} \quad (2.55)$$

$$D_{hw} = \frac{4A\alpha_w}{S_w} \quad (2.56)$$

3 Summary of The Two-Fluid Incompressible Models

3.1 Model I

Conservation of mass

$$\frac{\partial \beta}{\partial t} + \frac{\partial}{\partial x} \left(\frac{V (\beta - \rho_o)(\beta - \rho_w)}{\beta (\rho_o - \rho_w)} + u_m \beta \right) = 0 \quad (3.1)$$

Conservation of momentum

$$\frac{\partial V}{\partial t} + \frac{\partial}{\partial x} \left(\frac{V^2}{\beta^2} \frac{\beta^2 - \rho_o \rho_w}{2(\rho_o - \rho_w)} + u_m V + (\rho_o - \rho_w) g \cos \varphi h_w(\beta) \right) = q_v \quad (3.2)$$

$$q_v = \frac{\tau_{W_o}}{\alpha_o} \frac{S_o}{A} + \frac{\tau_{W_w}}{\alpha_w} \frac{S_w}{A} - \frac{\tau_i}{\alpha_o \alpha_w} \frac{S_i}{A} - (\rho_o - \rho_w) g \sin \varphi \quad (3.3)$$

Definitions and expressions

$$\beta = \rho_w \alpha_o + \rho_o \alpha_w \quad (3.4)$$

$$V = \rho_o u_o - \rho_w u_w - (\rho_o - \rho_w) u_m \quad (3.5)$$

$$u_o = u_m + \frac{V}{\beta} \alpha_w \quad (3.6)$$

$$u_w = u_m - \frac{V}{\beta} \alpha_o \quad (3.7)$$

$$\alpha_o = \frac{\beta - \rho_o}{\rho_w - \rho_o} \quad (3.8)$$

$$\alpha_w = \frac{\beta - \rho_w}{\rho_o - \rho_w} \quad (3.9)$$

$$\frac{V}{\beta} = u_s \quad (3.10)$$

3.1.1 Solution Strategy

$$u_m \xrightarrow{\text{impose}} \begin{bmatrix} \text{Conservation of mass} \\ \text{Conservation of Momentum} \end{bmatrix} \Rightarrow \begin{bmatrix} \beta \\ V \end{bmatrix} \Rightarrow \begin{bmatrix} \alpha_o & \alpha_w \\ u_o & u_w \end{bmatrix}$$

3.2 Model II

Conservation of mass

$$\frac{\partial \rho_m}{\partial t} + \frac{\partial}{\partial x} \left(\rho_m u_m - (\rho_w - \rho_o) \alpha_o \alpha_w u_s \right) = 0 \quad (3.11)$$

Conservation of momentum

$$\begin{aligned} \frac{\partial}{\partial t} (\rho_m - (\rho_w + \rho_o)) u_s + \frac{\partial}{\partial x} \left((\rho_w \alpha_o^2 - \rho_o \alpha_w^2) \frac{u_s^2}{2} - (\rho_w \alpha_o + \rho_o \alpha_w) u_s u_m + (\rho_w - \rho_o) g h_w \cos \beta \right) \\ = \frac{\tau_{W_o} S_o}{\alpha_o A} - \frac{\tau_{W_w} S_w}{\alpha_w A} + \frac{\tau_i S_i}{\alpha_o \alpha_w A} - (\rho_w - \rho_o) g \sin \beta \end{aligned} \quad (3.12)$$

Definitions and expressions

$$\rho_m = \alpha_w \rho_w + \alpha_o \rho_o \quad (3.13)$$

$$u_m = \alpha_w u_w + \alpha_o u_o \quad (3.14)$$

$$u_o = u_m + \alpha_w u_s \quad (3.15)$$

$$u_w = u_m - \alpha_o u_s \quad (3.16)$$

$$\alpha_o = \frac{\rho_w - \rho_m}{\rho_w - \rho_o} \quad (3.17)$$

$$\alpha_w = \frac{\rho_m - \rho_o}{\rho_w - \rho_o} \quad (3.18)$$

$$u_s = u_o - u_w \quad (3.19)$$

3.2.1 Solution Strategy

$$u_m \xrightarrow{\text{impose}} \begin{bmatrix} \text{Conservation of mass} \\ \text{Conservation of Momentum} \end{bmatrix} \Rightarrow \begin{bmatrix} \rho_m \\ u_s \end{bmatrix} \Rightarrow \begin{bmatrix} \alpha_o & \alpha_w \\ u_o & u_w \end{bmatrix}$$

4 Discretization and numerical solution

4.1 general numerical solution

By solving the derived models numerically, we will be able to find out their different behavior, and which terms in those equations are dominating the solution. This is followed by implementing an explicit scheme with both upwind and central discretization. The upwind scheme uses the biased differencing based on the direction of the characteristic velocity, in this case the mixture velocity, which is assumed positive to the right. First, a general numerical solution will be introduced and since both models are of the same structure, and then this methodology is applied to both models.

4.1.1 Grid

The pipe is divided by control volumes in a one dimensional uniform grid. Control volumes are separated by the boundaries. The first cell ($j = 1$) and the last cell ($j = imax + 2$) are virtual cells and are reserved for boundary conditions. The first cell's index is chosen to be 1 to be consistent with programming in Matlab. Considering the inlet of the pipe as $x = 0$ and the first actual cell inside the pipe as $j = 2$, the coordinates of the cell center (x_j) and cell faces ($x_{j+1/2}$) will be

$$x_j = (j - 1.5)\Delta x \quad (4.1)$$

$$x_{j+1/2} = (j - 1)\Delta x \quad (4.2)$$

The grid in time is also assumed uniform. The new time step is calculated from the old time step in the following manner

$$t_{n+1} = t_n + \Delta t \quad (4.3)$$

4.1.2 Discretization

The derived conservation equations in the previous sections have the general form

$$\frac{\partial U}{\partial t} + \frac{\partial f}{\partial x} = Q \quad (4.4)$$

We integrate the conservation equation within each control volume

$$\int_V \frac{\partial U}{\partial t} dV + \int_V \frac{\partial f}{\partial x} dV = \int_V Q dV \quad (4.5)$$

First, we start integrating the above equation in space. Using Green's theorem

$$\frac{\partial}{\partial t} \int_V U dV + \oint_S f \cdot \hat{n} dS = \int_V Q dV \quad (4.6)$$

The first integral on the left hand side, and the source term integral on the right hand side are evaluated by taking the average cell value at the cell center

$$\frac{\partial}{\partial t} (U_j \Delta x) + \left(f_{j+1/2}(\hat{i}) + f_{j-1/2}(-\hat{i}) \right) = Q_j \Delta x \quad (4.7)$$

$$\frac{\partial U_j}{\partial t} + \frac{f_{j+1/2} - f_{j-1/2}}{\Delta x} = Q_j \quad (4.8)$$

The advantage of using the finite volume method is that it is automatically conservative, as the outgoing flux of the one cell is the same as the ingoing flux of the adjacent cell. Evaluating the time derivative using Euler forward for both sources and fluxes

$$\frac{U_j^{n+1} - U_j^n}{\Delta t} + \frac{f_{j+1/2}^n - f_{j-1/2}^n}{\Delta x} = Q_j^n \quad (4.9)$$

This gives at the end an Euler forward, fully explicit scheme. This discretization will be applied to both models in the following sections.

4.1.3 Boundary condition

As explained earlier the first and the last cells are reserved for boundary conditions. However since the last cell is to the right of the pipe's outlet, the values assigned to this cell center are based on linear extrapolation instead of just assigning zero in order to avoid sharp and unrealistic changes in gradients. If we assume a conservative variable U_j at the last cell inside the pipe ($j = imax + 1$), the value assigned to the ghost-cell outside the pipe outlet becomes

$$U_{i_{max}+2} = 2U_{i_{max}+1} - U_{i_{max}} \quad (4.10)$$

4.2 Discretizing model I

We start by discretizing the conservation of mass equation (2.22) using the upwind finite difference scheme.

$$\frac{\partial \beta}{\partial t} + \frac{\partial}{\partial x} \underbrace{\left(\frac{V(\beta - \rho_o)(\beta - \rho_w)}{\beta(\rho_o - \rho_w)} \right)}_{f_\beta} = 0 \quad (4.11)$$

In the above equation the whole spatial derivative term is called f_β to be concise. In applying the upwind scheme, all of the terms in the spatial derivative (β and V) are evaluated using data points j and $j - 1$ over a fixed grid distance of Δx .

$$\frac{\beta_j^{n+1} - \beta_j^n}{\Delta t} + \frac{f_{\beta,j+\frac{1}{2}}^n - f_{\beta,j-\frac{1}{2}}^n}{\Delta x} = 0 \quad (4.12)$$

Where f_β at node j is evaluated at the old time step as the following

$$f_{\beta,j+\frac{1}{2}}^n = \frac{V_j^n (\beta_{j+\frac{1}{2}}^n - \rho_o)(\beta_{j+\frac{1}{2}}^n - \rho_w)}{\beta_{j+\frac{1}{2}}^n (\rho_o - \rho_w)} \quad (4.13)$$

Where $\beta_{j+\frac{1}{2}}$ is calculated at the face of the cells

$$\beta_{j+\frac{1}{2}} = \frac{1}{2}(\beta_j + \beta_{j+1}) \quad (4.14)$$

Using the central discretization for the reversed density β is recommended, because it makes the scheme stable. This is found from trial-and-error in this work, and there is also a direct reference

to this issue in [15]. Taking the density data from upstream and downstream avoids overfilling the cells numerically when transition from one phase to two-phase flow happens. Therefore, the new β (reverse density) at the new time step is calculated from the following algebraic equation.

$$\beta_j^{n+1} = \beta_j^n + \frac{\Delta t}{\Delta x} \left(f_{\beta,j-\frac{1}{2}}^n - f_{\beta,j+\frac{1}{2}}^n \right) \quad (4.15)$$

We move on to discretize the momentum equation (2.23) according to the same scheme

$$\frac{\partial V}{\partial t} + \frac{\partial}{\partial x} \left(\frac{V^2}{\beta^2} \frac{\beta^2 - \rho_o \rho_w}{2(\rho_o - \rho_w)} + u_m V + (\rho_o - \rho_w) g \cos \varphi h_w \right) = q_v \quad (4.16)$$

$$\frac{V_j^{n+1} - V_j^n}{\Delta t} + \frac{f_{V,j+\frac{1}{2}}^n - f_{V,j-\frac{1}{2}}^n}{\Delta x} = q_v \quad (4.17)$$

Where the momentum flux, $f_{V,j}^n$ is defined as

$$f_{V,j+\frac{1}{2}}^n = \frac{(V_j^n)^2}{(\beta_{j+1/2}^n)^2} \frac{(\beta_{j+1/2}^n)^2 - \rho_o \rho_w}{2(\rho_o - \rho_w)} + u_m (V_j^n) + (\rho_o - \rho_w) g \cos \varphi h_{w,j+1/2}^n \quad (4.18)$$

The momentum flux consists of three terms. The first term $\frac{V^2}{\beta^2} \frac{\beta^2 - \rho_o \rho_w}{2(\rho_o - \rho_w)}$ which is interpreted as transport due to mixture velocity. It plays an important role in transition from one-phase to two-phase flow. The discretization of this term should be in a way that allows a smooth transition in each cell filled with one phase to two phases. Wrong discretization will lead to overfilling the cell with the same phase and negative phase fraction with the other cell, which result in exploding the numerical scheme. Trial and error on different solutions has shown that the mixture density (the reverse density) gives the stable solution when defined on the cell faces.

The level gradient also needs information from the upstream and downstream of the cell. So a central discretization is also considered here

$$h_{w,j+1/2}^n = \frac{1}{2} (h_{w,j+1}^n + h_{w,j}^n) \quad (4.19)$$

We get the new V (momentum slip) from the following algebraic equation

$$V_j^{n+1} = V_j^n + \Delta t \left(\frac{f_{V,j-\frac{1}{2}}^n - f_{V,j+\frac{1}{2}}^n}{\Delta x} + q_v \right) \quad (4.20)$$

This dynamic model calculates the new V as a function of old values of β and V

$$V^{n+1} = V(\beta^n, V^n) \quad (4.21)$$

By solving the two algebraic equations (4.15) and (4.20), we can solve for β and V over the whole grid by using the initial and boundary conditions. The first node on the grid is a ghost point and is dedicated to the boundary condition at all the time steps. We determine also the initial condition for all the nodes at $t = 0$. The time step used further in this work is in most cases $dt = 0.005[s]$ and for high mixture velocities $dt = 0.001[s]$. Any bigger time step resulted in numerical instability of the scheme. A more thorough discussion is followed in section 5.4

4.3 Model I-steady state discretization

In the previous part we have used the momentum equation (2.23) to calculate V and therefore calculate the slip velocity. If we decide to neglect the acceleration terms in the momentum equation, we get the steady state slip relation. Using the same discretization method for the mass equation, the new β is used in the steady state holdup equation to calculate the V at the new time step. To sum up, we are solving one simple algebraic equation and one nonlinear equation

$$\beta_j^{n+1} = \beta_j^n + \frac{\Delta t}{\Delta x} (f_{\beta,j-1}^n - f_{\beta,j}^n) \quad (4.22)$$

$$0 = \frac{\tau_{W_o} S_o}{\alpha_o A_o} + \frac{\tau_{W_w} S_w}{\alpha_w A_w} - \frac{\tau_i S_i}{\alpha_o \alpha_w A_i} - (\rho_o - \rho_w)g \sin \varphi - (\rho_o - \rho_w)g \frac{\partial h_w}{\partial x} \cos \varphi \quad (4.23)$$

We use the new β in the equation (4.23) to calculate the new corresponding V . In other words at each time step the variable V is the function of β

$$V = V(\beta^n) \quad (4.24)$$

At the end the effect of the dynamic and steady state slip relations on the final solution are compared.

4.4 Discretizing model II

First the mass conservation equation (3.11) is discretized according to numerical solution explained at the beginning.

$$\frac{\partial \rho_m}{\partial t} + \frac{\partial}{\partial x} (\rho_m u_m - (\rho_w - \rho_o) \alpha_o \alpha_w u_s) = 0 \quad (4.25)$$

$$\frac{\rho_{m,j}^{n+1} - \rho_{m,j}^n}{\Delta t} + \frac{f_{\rho,j+1/2}^n - f_{\rho,j-1/2}^n}{\Delta x} = 0 \quad (4.26)$$

$$f_{\rho,j+1/2}^n = \rho_{m,j}^n u_m - (\rho_w - \rho_o) \alpha_{o,j+1/2}^n \alpha_{w,j+1/2}^n u_{s,j}^n \quad (4.27)$$

$$\rho_{m,j}^{n+1} = \rho_{m,j}^n + \frac{\Delta t}{\Delta x} (f_{\rho,j-1/2}^n - f_{\rho,j+1/2}^n) \quad (4.28)$$

Fluxes at the face cells are defined as a function of average mixture density on the face cells and the slip velocity at the cell centers. The concept of average density at the face cells is hidden in the variables: void fractions, which are functions of the average density. This is (similar to the first model) due to avoiding the negative phase fractions in the cells when transition from one-phase to two-phase flow takes place.

$$\alpha_{o,j+1/2}^n = \frac{\rho_w - \rho_{m,j+1/2}^n}{\rho_w - \rho_o} \quad (4.29)$$

$$\alpha_{w,j+1/2}^n = \frac{\rho_{m,j+1/2}^n - \rho_o}{\rho_w - \rho_o} \quad (4.30)$$

$$\rho_{m,j+1/2}^n = \frac{1}{2} (\rho_{m,j+1}^n + \rho_{m,j}^n) \quad (4.31)$$

Now the momentum equation (3.12) is accordingly discretized

$$\frac{(\rho_{m,j}^{n+1} - (\rho_w - \rho_o)) u_{s,j}^{n+1} - (\rho_{m,j}^n - (\rho_w - \rho_o)) u_{s,j}^n}{\Delta t} + \frac{f_{u,j+1/2}^n - f_{u,j-1/2}^n}{\Delta x} = q_s \quad (4.32)$$

Where q_s is the abbreviation of the source term

$$q_s = \frac{\tau_{W_o} S_o}{\alpha_o A} - \frac{\tau_{W_w} S_w}{\alpha_w A} + \frac{\tau_i S_i}{\alpha_o \alpha_w A} - (\rho_w - \rho_o) g \sin \varphi \quad (4.33)$$

Moreover, the momentum flux at the cell faces consists of two terms related to mixture slip and one term related to level gradient. Also in the momentum flux, the mixture density is calculated at the cell face as an average value of the two adjacent cell centers.

$$f_{u,j+1/2}^n = \left(\rho_w \alpha_o^2_{o,j+1/2} - \rho_o \alpha_w^2_{w,j-1/2} \right) \frac{u_s^2}{2} - (\rho_w \alpha_o_{o,j+1/2} + \rho_o \alpha_w_{w,j+1/2}) u_m u_{s,j} \quad (4.34)$$

$$+ (\rho_o - \rho_w) g h_{w,j+1/2} \cos \varphi \quad (4.35)$$

Finally, the slip velocity is calculated from the equation below, which is an algebraic equation. The value of the mixture density at the new time step is calculated first from the conservation of mass equation and then substituted in this equation

$$u_{s,j}^{n+1} = \frac{1}{(\rho_{m,j}^{n+1} - (\rho_w - \rho_o))} \left((\rho_{m,j}^n - (\rho_w - \rho_o)) u_{s,j}^n + \Delta t \left(\frac{f_{u,j-1/2}^n - f_{u,j+1/2}^n}{\Delta x} + q_s \right) \right) \quad (4.36)$$

4.5 Model II-steady state discretization

For deriving the steady-state model, we simplify the equations by neglecting the acceleration terms, which leaves us with the following system of equations

$$\rho_{m,j}^{n+1} = \rho_{m,j}^n + \frac{\Delta t}{\Delta x} \left(f_{\rho,j-1/2}^n - f_{\rho,j+1/2}^n \right) \quad (4.37)$$

$$0 = \frac{\tau_{W_o} S_o}{\alpha_o A} - \frac{\tau_{W_w} S_w}{\alpha_w A} + \frac{\tau_i S_i}{\alpha_o \alpha_w A} - (\rho_w - \rho_o) g \sin \varphi - (\rho_w - \rho_o) g \frac{\partial h_w}{\partial x} \cos \varphi \quad (4.38)$$

5 Validating the model and sensitivity analysis

After implementing the models numerically in Matlab, several cases have been chosen to compare the dynamic solution with the stationary solution. We can change many parameters and conduct this study. We have chosen horizontal pipe with varying mixture velocity for the first case study. The second case study is about to keep the mixture velocity constant and the pipe angle changes. If the dynamic and stationary solutions are indeed different, we are able to see these differences in these cases, and predict under which circumstances these differences become significant.

5.1 Sensitivity analysis on mixture velocity for horizontal pipes

5.1.1 Model I

The sensitivity analysis carried out on the model I for horizontal pipe, starts from low to high mixture velocities. The first two plots belong to the dynamic model only and depict how the changes in the mixture velocity affect the rate of flushing and the relation between water holdup and the watercut. The acceleration is expected not to be considerable factor for low mixture velocity. The dominating term in the momentum equation for low mixture velocities turns out to be the level gradient. As the mixture velocity increases, the acceleration terms begin to become more and more significant to the same order of magnitude as the level gradient.

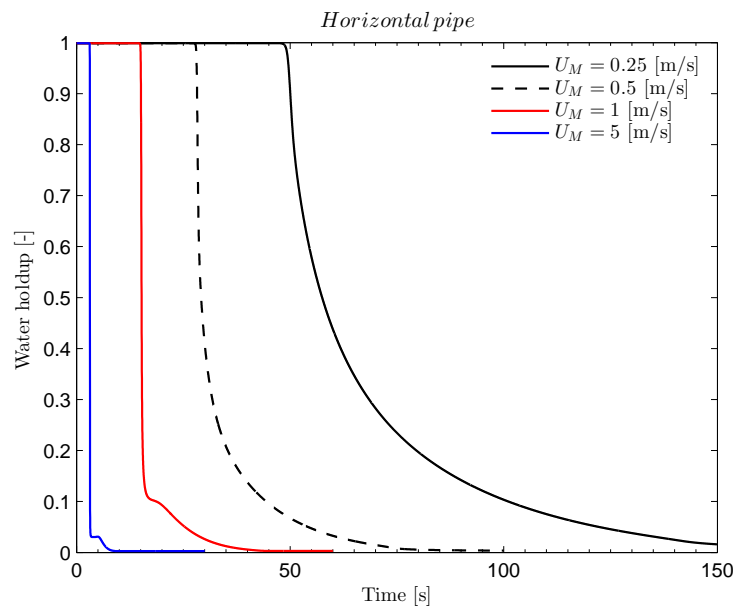


Figure 3: Effect of different mixture velocities on the flushing rate of water with oil in the dynamic model

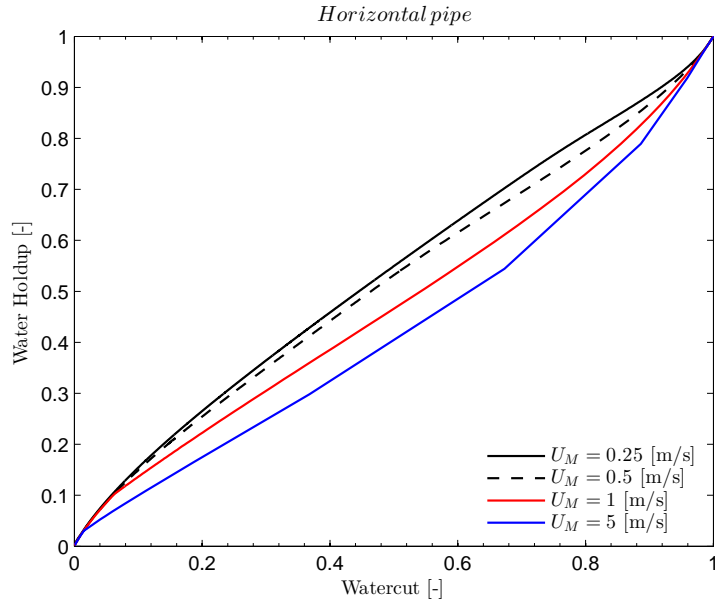


Figure 4: Relation between water holdup and the watercut as a function of mixture velocity in a horizontal pipe

The rest of the figures illustrate oil and water holdup, of both dynamic and stationary solutions, changing with time as the mixture velocity is increasing. The dynamic and the stationary solutions show good agreement at low mixture velocities, almost identical. However, with increasing the velocity, the solutions start to deviate more. The dynamic solutions shows a sharper oil holdup changes as opposed to the stationary solution. Two important points should be mentioned as the main factors that cause this difference.

The acceleration is expected not to be a considerable factor for low mixture velocity. The dominating term in the momentum equation for low mixture velocities turns out to be the level gradient. To sum up

- The acceleration terms in the dynamic model are not significant for low mixture velocities. The dominating term in the momentum equation for low mixture velocities is the level gradient. This will be discussed in more details in chapter 6.
- As the mixture velocity increases the acceleration terms begin to become more and more significant to the same order of magnitude as the level gradient.

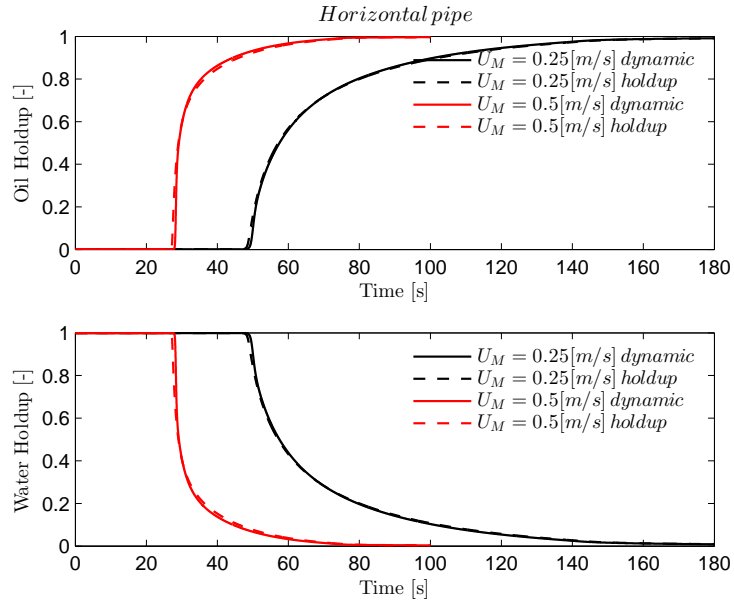


Figure 5: Oil and water holdups at the pipe outlet for $U_M < 1$

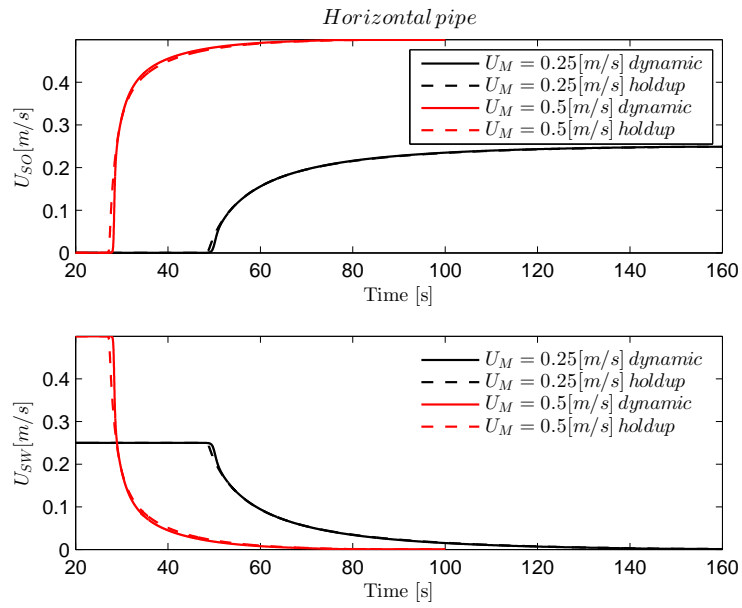


Figure 6: Oil and water superficial velocities at the pipe outlet for $U_M < 1$

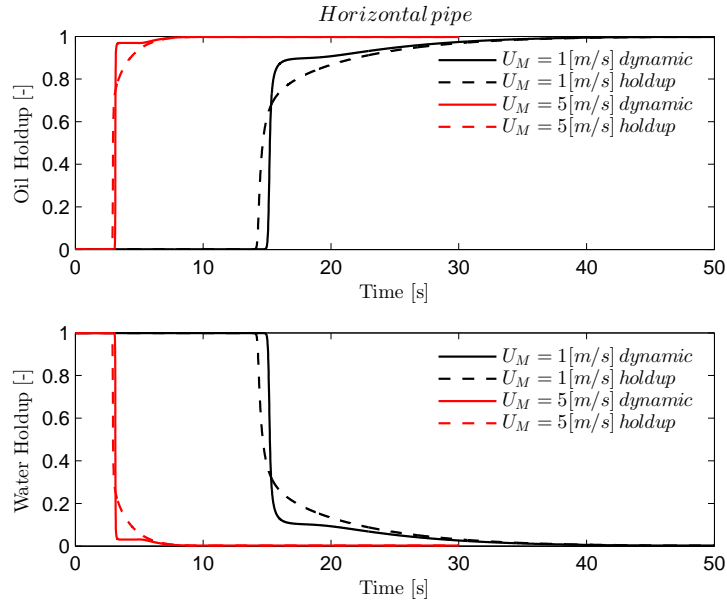


Figure 7: Oil and water holdups at the pipe outlet for $U_M > 1$

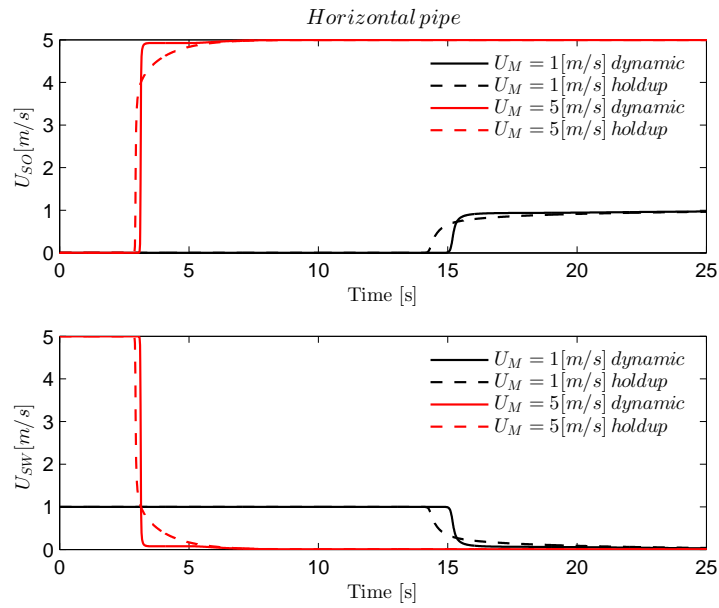


Figure 8: Oil and water superficial velocities at the pipe outlet for $U_M < 1$

5.1.2 Model II

The same sensitivity analysis is carried on model II for horizontal pipes. In principle, it is expected that the two models should give the same result. We get a confirmation on this throughout this section. Similar to the previous section, the analysis moves from the low mixture velocities to high velocities, and the results are compared with each other. The same main two points also apply for this model.

- The acceleration terms in the dynamic model are not significant for low mixture velocities. The dominating term in the momentum equation for low mixture velocities turns out to be the level gradient. This will be discussed in more details in chapter 6.
- As the mixture velocity increases the acceleration terms begin to become more and more significant to the same order of magnitude as the level gradient.

These two models have shown similar behavior so far, as expected.

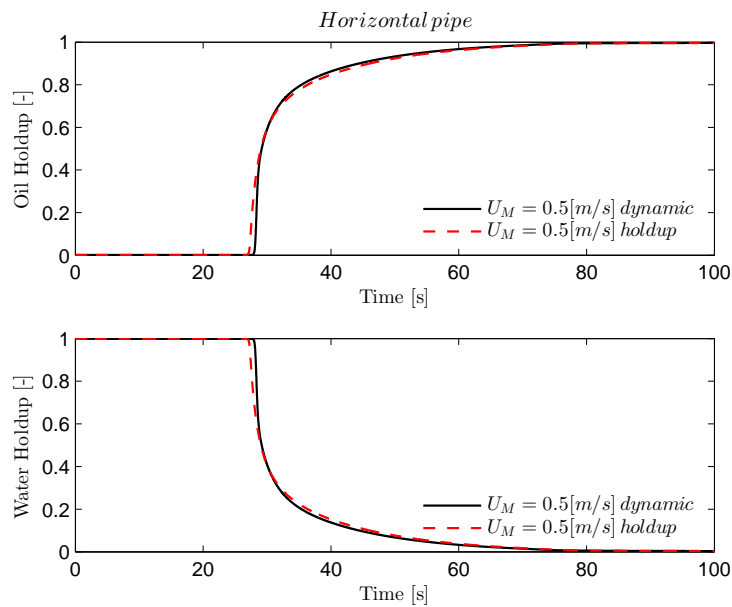


Figure 9: Oil and water holdups at the pipe outlet for $U_M < 1$

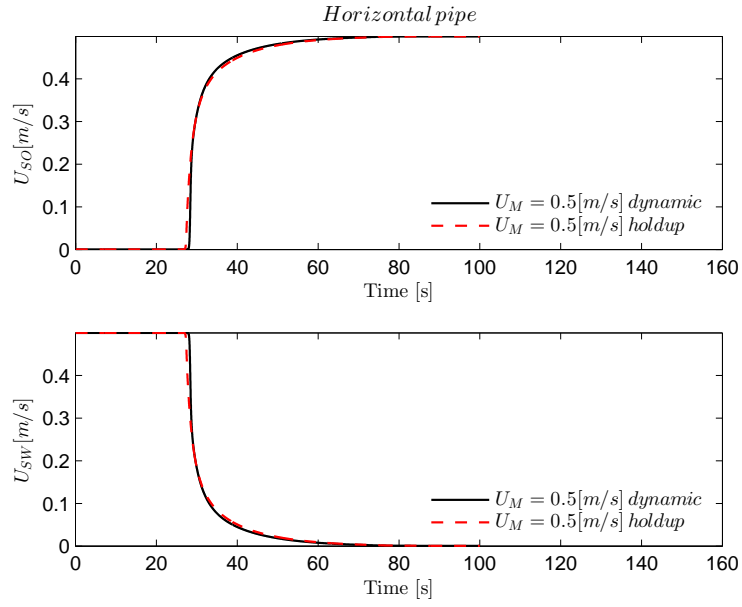


Figure 10: Oil and water superficial velocities at the pipe outlet for $U_M < 1$

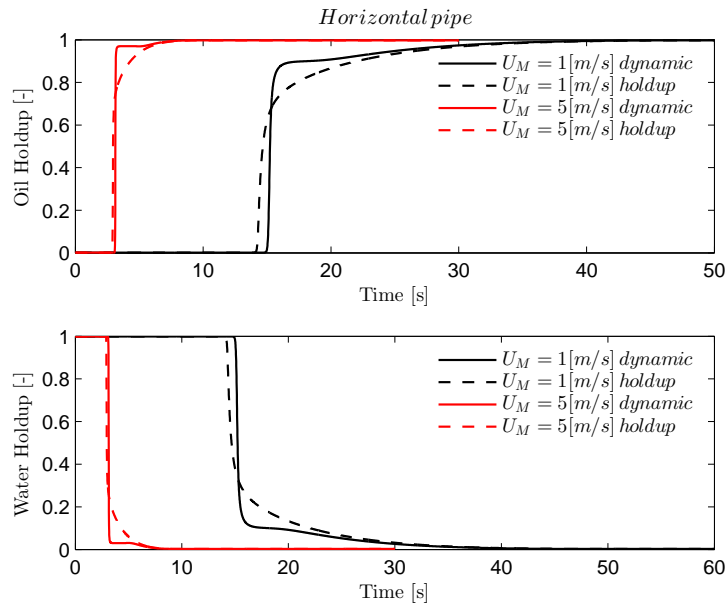


Figure 11: Oil and water holdups at the pipe outlet for $U_M > 1$

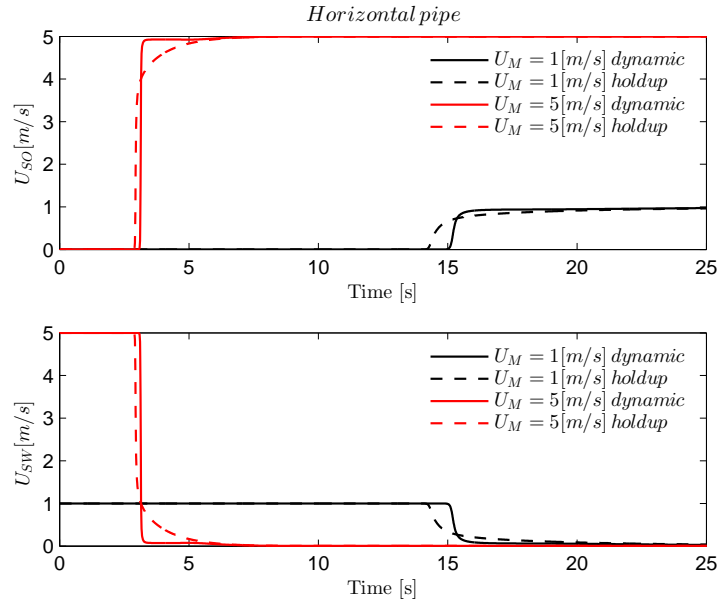


Figure 12: Oil and water superficial velocities at the pipe outlet for $U_M > 1$

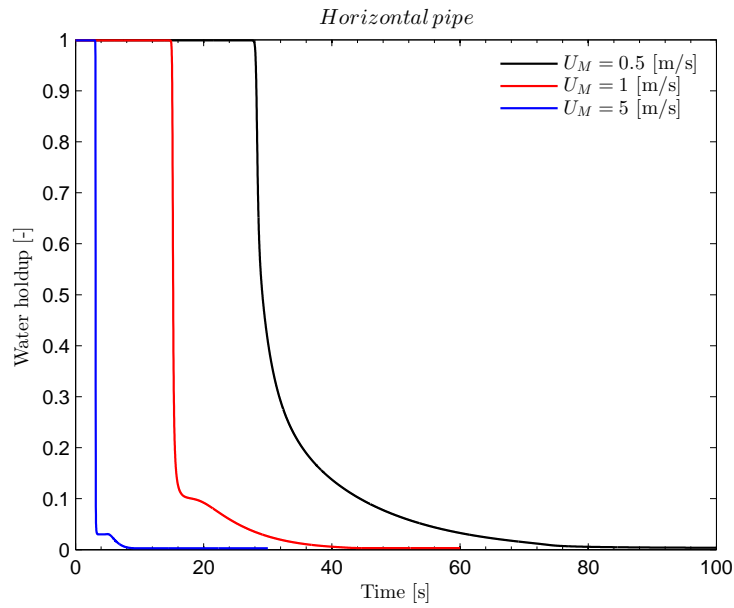


Figure 13: Effect of different mixture velocities on the flushing rate of water with oil in the dynamic model

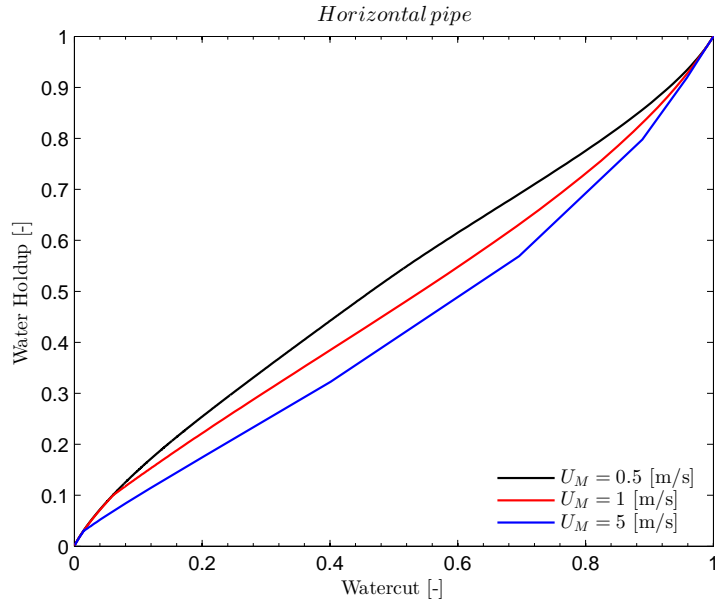


Figure 14: Relation between water holdup and the watercut as a function of mixture velocity in a horizontal pipe

The results for both models confirm that the dynamic models introduce a sharper oil front compared to the holdup equation. This becomes more important when the mixture velocity increases.

5.2 Sensitivity analysis on pipe angle

The second case study looks at the differences between the dynamic and stationary solutions that rise due to the change of pipe angle. When the pipe is not horizontal anymore, the gravity starts to act on the flow. Gravity influences the rate at which flushing occurs. The mixture velocity for all the cases is set to be $U_M = 0.5 [m/s]$ and the angle changes from $+5$ to -5 degrees.

5.2.1 Model I

In this section Model I is put to test by varying the inclination from 5 to -5 degrees. The following plots confirm that the difference for positive inclinations is considerable. For negative inclinations, the solutions are almost identical.

It should be noted that all the plots are drawn in a way, that the upper part of the plot illustrates the oil holdup at the beginning of the pipe at $x = 1[m]$ and the lower plot shows the oil holdup at the pipe's outlet at $x = 16[m]$.

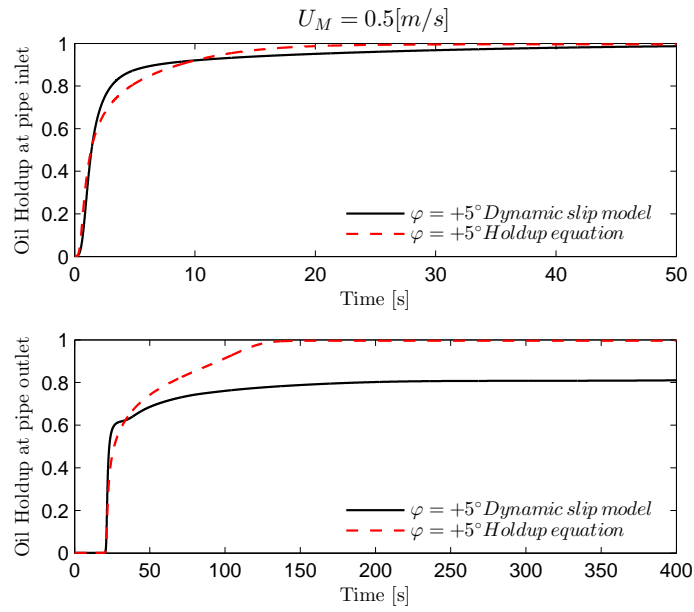


Figure 15: Oil holdup at the inlet/outlet of a 5° inclined pipe

+5 degrees inclination seems to be an extreme case where the dynamic model fails to flush out the water completely in the period that the steady state model does. This is probably a limitation for the dynamic model at this angle that cannot flush the water completely. When the angle is increased positively, the dynamic and holdup solutions deviate from one another at the points where the oil front hits the water.

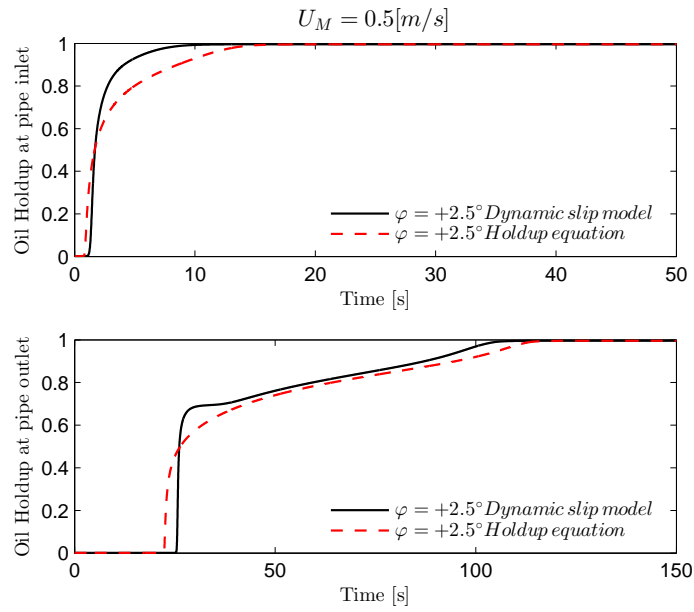


Figure 16: Oil holdup at the inlet/outlet of a 2.5° inclined pipe

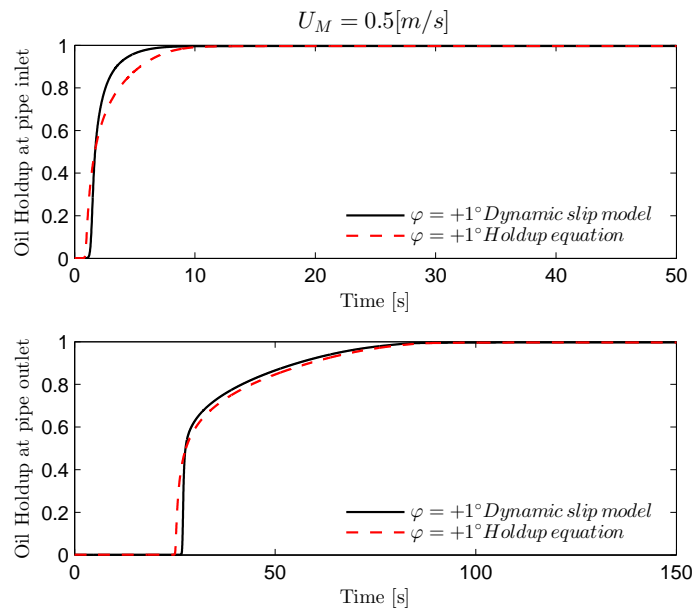


Figure 17: Oil holdup at the inlet/outlet of a 1° inclined pipe

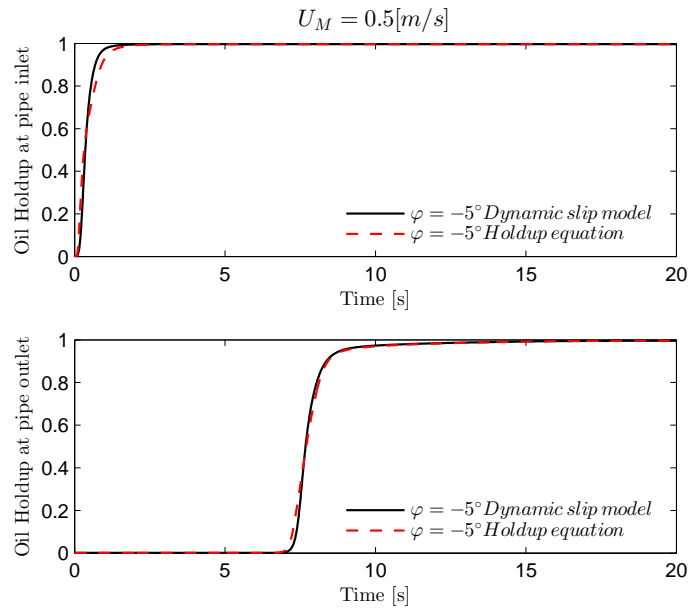


Figure 18: Oil holdup at the inlet/outlet of a -5° inclined pipe

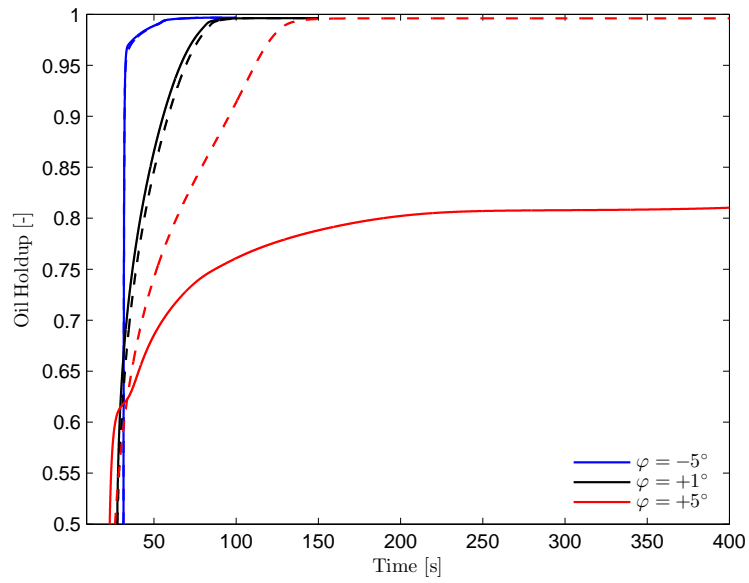


Figure 19: Pipe inclination effect on the oil holdup for $U_M = 0.5$, the dynamic model

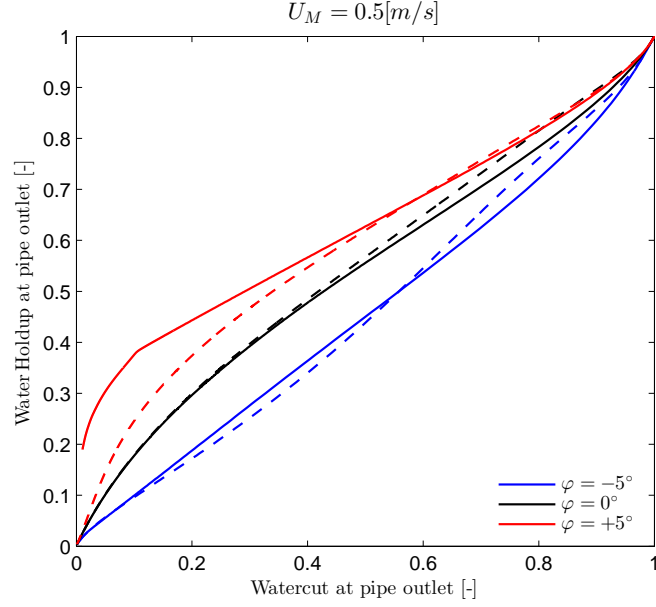


Figure 20: Watercut changes as a function of pipe angle for $U_M = 0.5$ at pipe outlet

The reason that the continuous red line has not been drawn all the way to the point zero, is that the dynamic model, has not managed to flush out the water completely.

If we look at the dynamic model again

$$\frac{\partial V}{\partial t} + \frac{\partial}{\partial x} \left(\frac{V^2}{\beta^2} \frac{\beta^2 - \rho_o \rho_w}{2(\rho_o - \rho_w)} + u_m V + (\rho_o - \rho_w) g \cos \varphi h_w(\beta) \right) = q_v \quad (5.1)$$

$$q_v = \frac{q_1}{\alpha_o} - \frac{q_2}{\alpha_w} = \frac{\tau_{W_o}}{\alpha_o} \frac{S_o}{A_o} + \frac{\tau_{W_w}}{\alpha_w} \frac{S_w}{A_w} - \frac{\tau_i}{\alpha_o \alpha_w} \frac{S_i}{A_i} - (\rho_o - \rho_w) g \sin \varphi \quad (5.2)$$

and the holdup equation

$$\frac{\tau_{W_o}}{\alpha_o} \frac{S_o}{A_o} + \frac{\tau_{W_w}}{\alpha_w} \frac{S_w}{A_w} - \frac{\tau_i}{\alpha_o \alpha_w} \frac{S_i}{A_i} - (\rho_o - \rho_w) g \sin \varphi = 0 \quad (5.3)$$

,it is noteworthy to mention that the gravity term appears in both models. So the reason that still these two solutions are not the same, is that the acceleration terms (forces) need to come in balance with all the forces in the right hand side of the equation including the gravity terms. The main reason is still lies in the acceleration terms, which in this case are affected by gravity as well.

5.2.2 Model II

As in the previous sections, the very similar case study is repeated for the second models. So far, the models have shown great agreement in behavior, and the following figures are also in accordance with the latter conclusion.

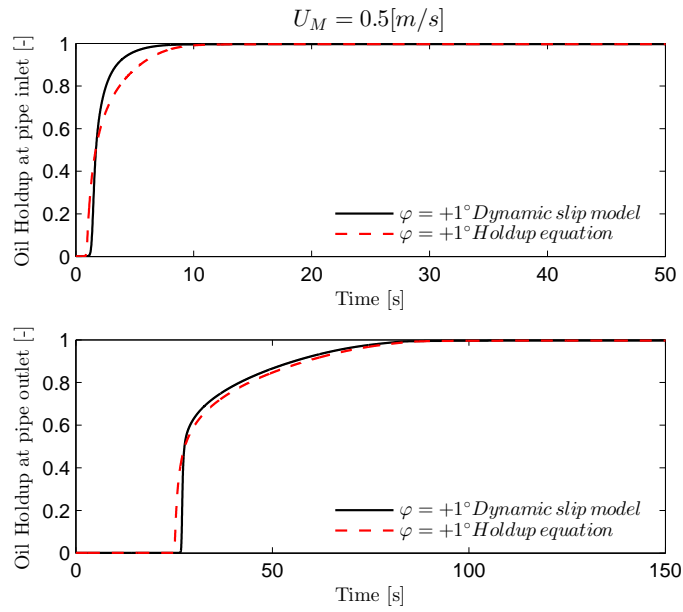


Figure 21: Oil holdup at the inlet/outlet of a 1° inclined pipe

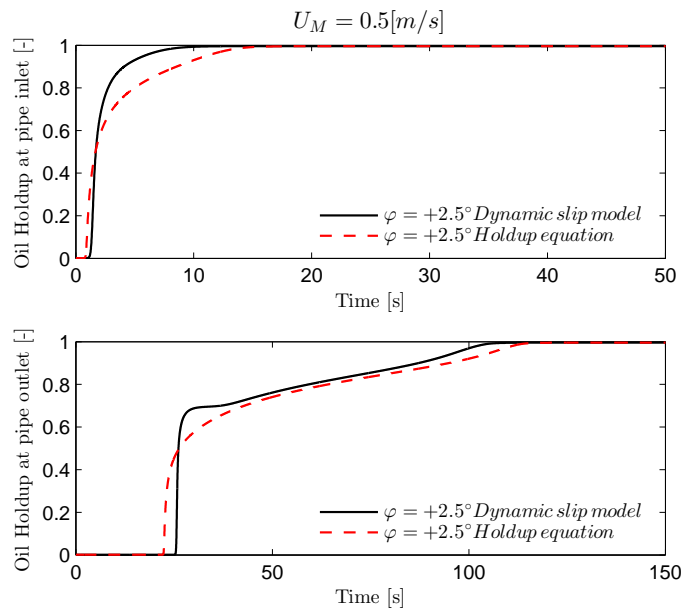


Figure 22: Oil holdup at the inlet/outlet of a 2.5° inclined pipe

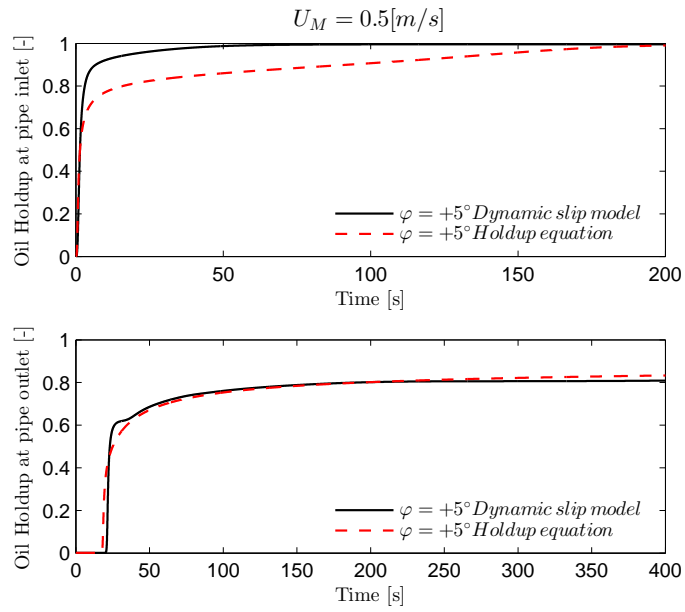


Figure 23: Oil holdup at the inlet/outlet of a 5° inclined pipe

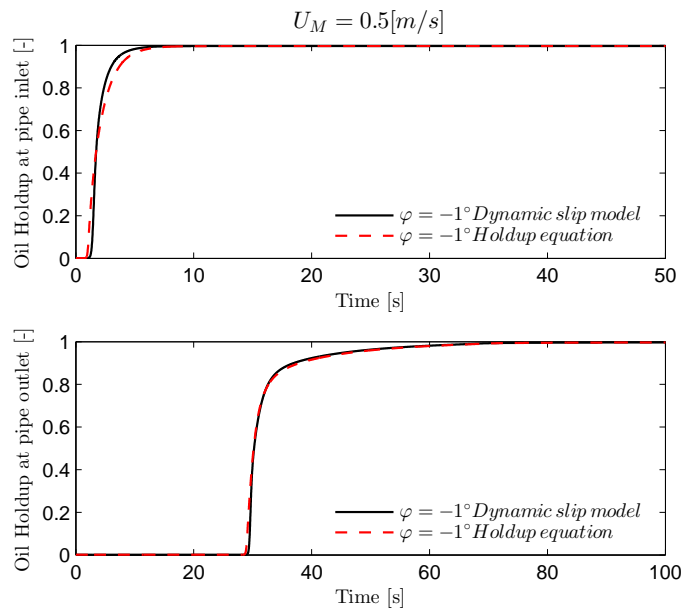


Figure 24: Oil holdup at the inlet/outlet of a -1° inclined pipe

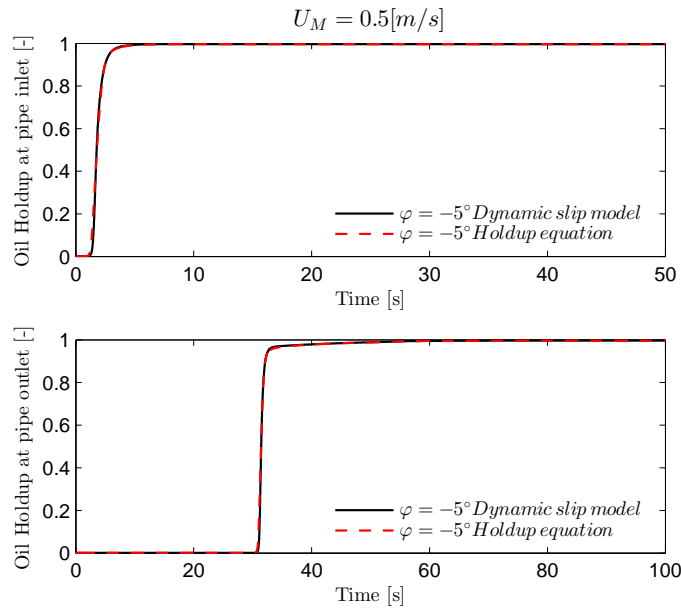


Figure 25: Oil holdup at the inlet/outlet of a -5° inclined pipe

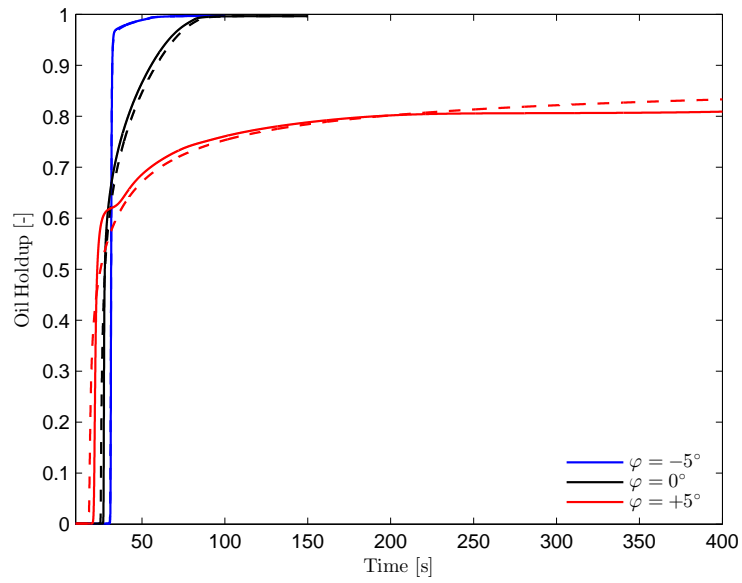


Figure 26: Pipe inclination effect on the oil holdup for $U_M = 0.5$

5.3 Model Limitations

The limitation of both models I and II lies in the source terms. There is a mathematical singularity at any phase fraction equal to zero, which means either oil, or water. If we look at the source term

$$q_s = \frac{\tau_{W_o} S_o}{\alpha_o A_o} + \frac{\tau_{W_w} S_w}{\alpha_w A_w} - \frac{\tau_i S_i}{\alpha_o \alpha_w A_i} - (\rho_o - \rho_w)g \sin \varphi$$

,it is obvious that neither α_o nor α_w can be absolute zero because they appear in the denominators in the source term. So the volume fractions for the case of one phase flow should be artificially set to zero, which means an α with order of magnitude 10^{-3} or less. Moreover, when a cell starts to fill with a second phase and is at a transition point between one phase to two-phase flow, the very small values of α 's at the denominators may cause the friction forces to grow nonphysically. The example below shows these forces in case of $U_M = 1[m/s]$, 2 meters from the pipe inlet.

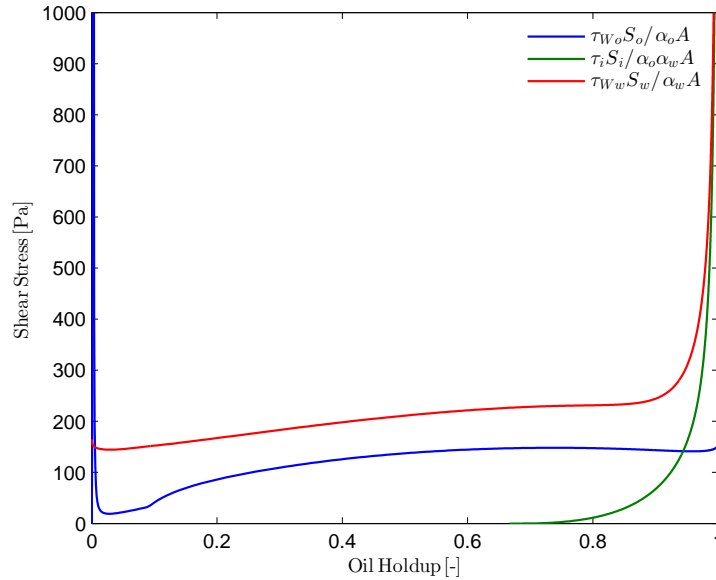


Figure 27: Oil wall shear stress changes compared to water and interface shear stress

The figures above show how the shear stress changes with respect to oil holdup changes.

5.4 Grid sensitivity in space and time

The grid study determines when the numerical solution converges as we increase the number of cells. This study has been done with the mixture velocity of $U_M = 0.5[m/s]$, and the results are taken at the pipe's outlet. From the figure below, it is obvious that the answer has already converged for 320 cells, and the answer is almost identical to 1600 cell's solution. Therefore, we have chosen 320 cells as the basis for the simulations.

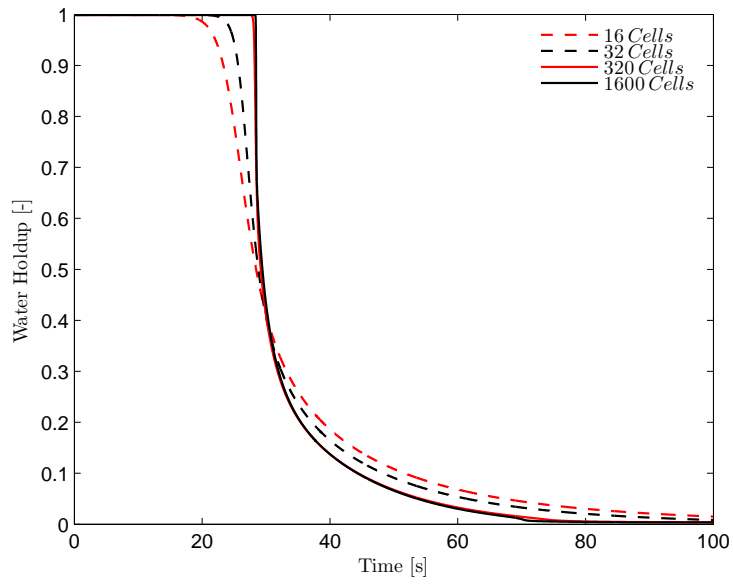


Figure 28: Water holdup solutions from coarse to fine grid

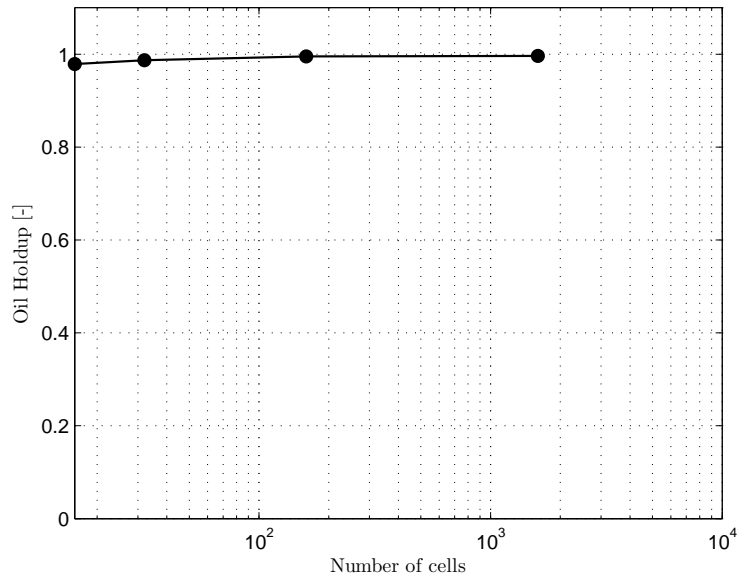


Figure 29: Grid study, oil holdup at 90 seconds after flushing starts

Solution at 90 seconds				
Number of cells	1600	160	32	16
α_o	0.9963	0.9951	0.9869	0.9789
Relative error	-	0.001204	0.009435	0.017465

The number of cells used for this case study is 320 cells, which was just discussed in the grid study. The largest time step used here is $dt = 0.005$. The time step used for high mixture velocity was reduced to $dt = 0.001$ with trial-and-error to overcome the instability of the scheme at high mixture velocities. Any bigger time step made the scheme unstable. The answer is well converged for all the time steps as shown figure 30

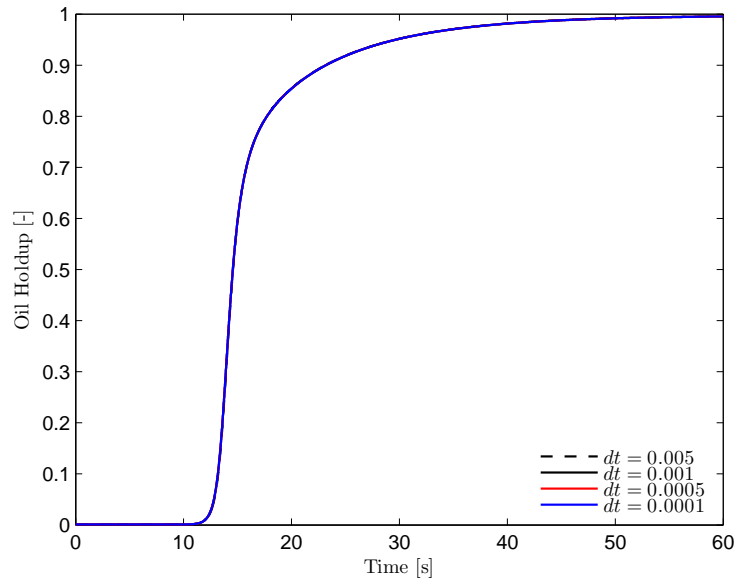


Figure 30: Grid sensitivity in time

6 Discussion

6.1 Comparison the magnitude of the terms in the momentum equations for oil and water

Due to the minor difference between the dynamic model and the holdup equations in some cases, it is important to have a closer look at each term in the governing equations to see which one dominates the solution. The discussion begins with equation (2.12). The two momentum equations show the balance between the pressure drop in each layer and the rest of forces. Two points have been chosen, one at the pipe inlet (at $x = 1[m]$) and the other one at the pipe outlet ($x = 16[m]$). Rearranging the equation (2.12), we can gather pressure force on the left side, and all the other forces on the right hand side of the equation. The result becomes

$$\alpha_o \frac{\partial p}{\partial x} = q_1 - \alpha_o \frac{\partial}{\partial t}(\rho_o u_o) + \alpha_o \frac{\partial}{\partial x} \left(\frac{1}{2} \rho_o u_o^2 \right) - \rho_o \alpha_o g \frac{\partial h_w}{\partial x} \cos \beta \quad (6.1)$$

$$\alpha_w \frac{\partial p}{\partial x} = q_2 - \alpha_w \frac{\partial}{\partial t}(\rho_w u_w) + \alpha_w \frac{\partial}{\partial x} \left(\frac{1}{2} \rho_w u_w^2 \right) - \rho_w \alpha_w g \frac{\partial h_w}{\partial x} \cos \beta \quad (6.2)$$

Where the source terms are

$$q_1 = -\frac{\tau_{W_o} S_o}{A} - \frac{\tau_i S_i}{A} \quad (6.3)$$

$$q_2 = -\frac{\tau_{W_w} S_w}{A} + \frac{\tau_i S_i}{A} \quad (6.4)$$

The right hand side of both equations include wall shear stress, shear stress at the interface, temporal and spatial derivatives and the level gradient. The sum of the forces on the left hand side balances the pressure force on the left hand side. This comparison case includes f cases with different mixture velocities. In each case, the first plot illustrates the pressure forces on oil and water layer, which is the left hand side of the momentum equation. The next two plots include the other forces balancing the pressure forces that is the left hand side of the momentum equations. Having plotted all these forces together, we can see which ones have a greater order of magnitude and therefore, dominate the solution.

6.1.1 Case I: $U_M = 0.25$

Plotting the left hand side of the momentum equations

$$\alpha_o \frac{\partial p}{\partial x} = \dots$$

$$\alpha_w \frac{\partial p}{\partial x} = \dots$$

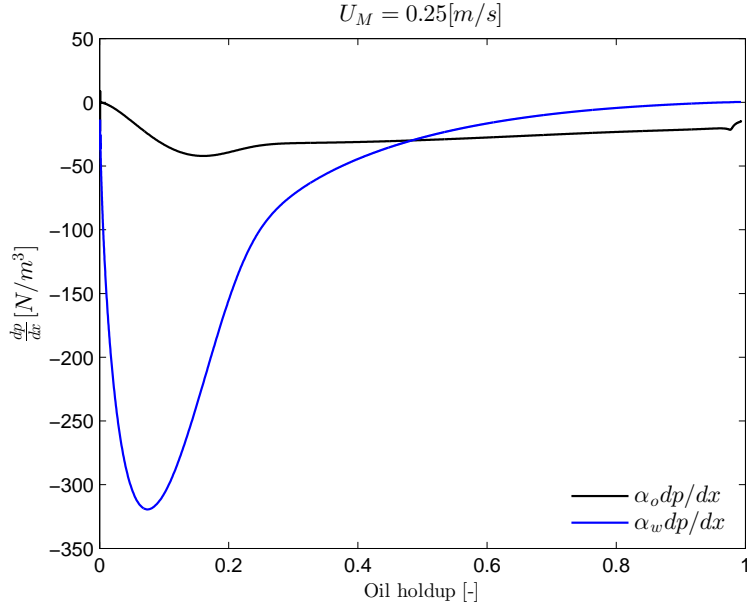


Figure 31: Pressure forces for oil and water layers, at $x = 16[m]$, $U_M = 0.25$

Plotting all the terms on the right hand side of the momentum equations

$$\dots = -\frac{\tau_{W_o} S_o}{A} - \frac{\tau_i S_i}{A} - \alpha_o \frac{\partial}{\partial t} (\rho_o u_o) + \alpha_o \frac{\partial}{\partial x} \left(\frac{1}{2} \rho_o u_o^2 \right) - \rho_o \alpha_o g \frac{\partial h_w}{\partial x} \cos \beta$$

$$\dots = -\frac{\tau_{W_w} S_w}{A} + \frac{\tau_i S_i}{A} - \alpha_w \frac{\partial}{\partial t} (\rho_w u_w) + \alpha_w \frac{\partial}{\partial x} \left(\frac{1}{2} \rho_w u_w^2 \right) - \rho_w \alpha_w g \frac{\partial h_w}{\partial x} \cos \beta$$

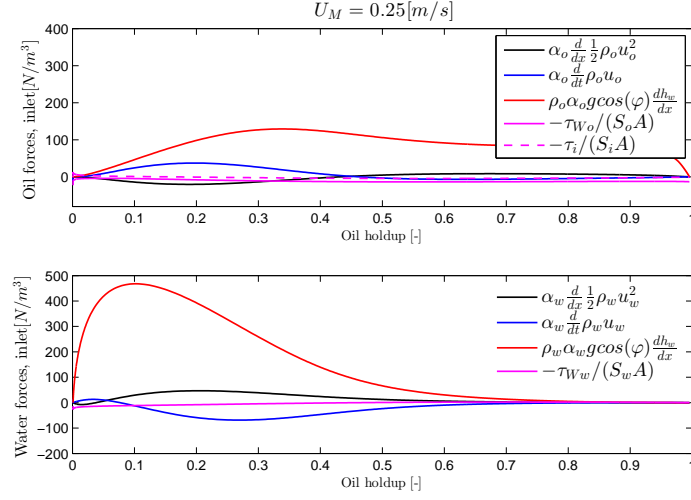


Figure 32: Oil momentum equation terms (top figure) and water (bottom figure), at $x = 1[m]$ with $U_M = 0.25$

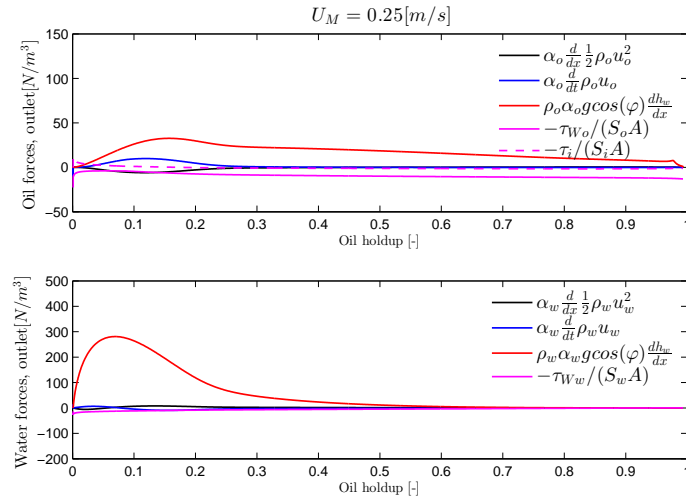


Figure 33: Oil momentum equation terms (top figure) and water (bottom figure), at $x = 16[m]$ with $U_M = 0.25$

6.1.2 Case II: $U_M = 0.5$

Plotting the left hand side of the momentum equations

$$\alpha_o \frac{\partial p}{\partial x} = \dots$$

$$\alpha_w \frac{\partial p}{\partial x} = \dots$$

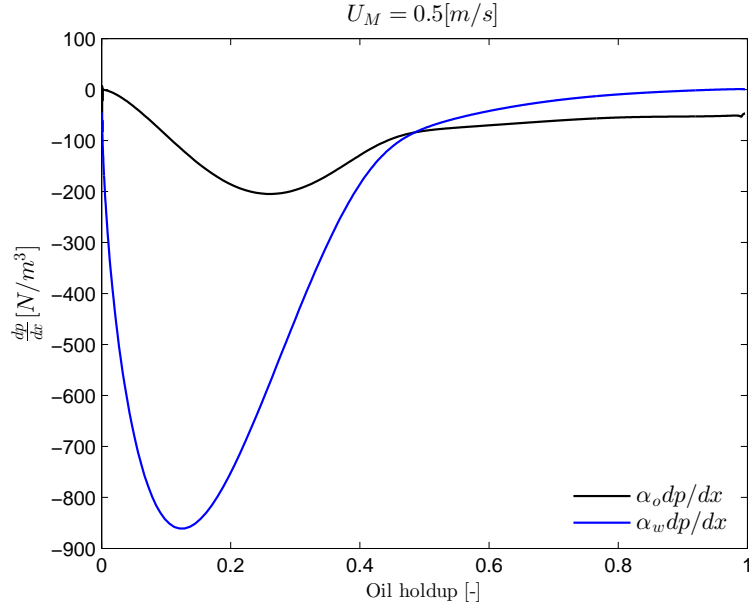


Figure 34: Pressure forces for oil and water layers, at $x = 16[m]$, $U_M = 0.5$

Plotting all the terms on the right hand side of the momentum equations

$$\dots = -\frac{\tau_{W_o} S_o}{A} - \frac{\tau_i S_i}{A} - \alpha_o \frac{\partial}{\partial t} (\rho_o u_o) + \alpha_o \frac{\partial}{\partial x} \left(\frac{1}{2} \rho_o u_o^2 \right) - \rho_o \alpha_o g \frac{\partial h_w}{\partial x} \cos \beta$$

$$\dots = -\frac{\tau_{W_w} S_w}{A} + \frac{\tau_i S_i}{A} - \alpha_w \frac{\partial}{\partial t} (\rho_w u_w) + \alpha_w \frac{\partial}{\partial x} \left(\frac{1}{2} \rho_w u_w^2 \right) - \rho_w \alpha_w g \frac{\partial h_w}{\partial x} \cos \beta$$

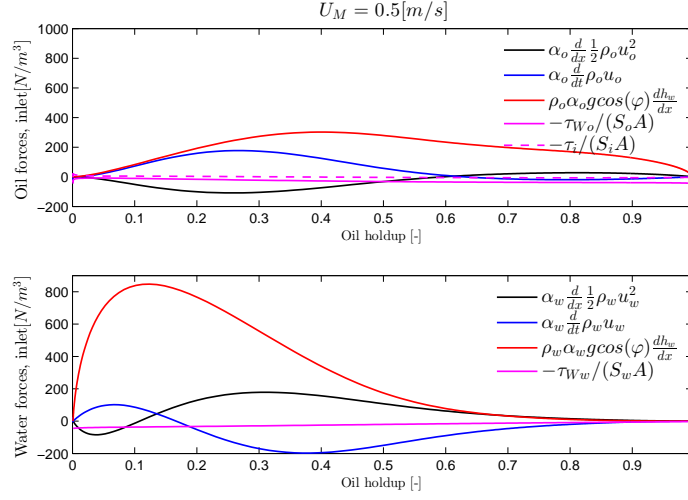


Figure 35: Oil momentum equation terms (top figure) and water (bottom figure), at $x = 1[m]$ with $U_M = 0.5$

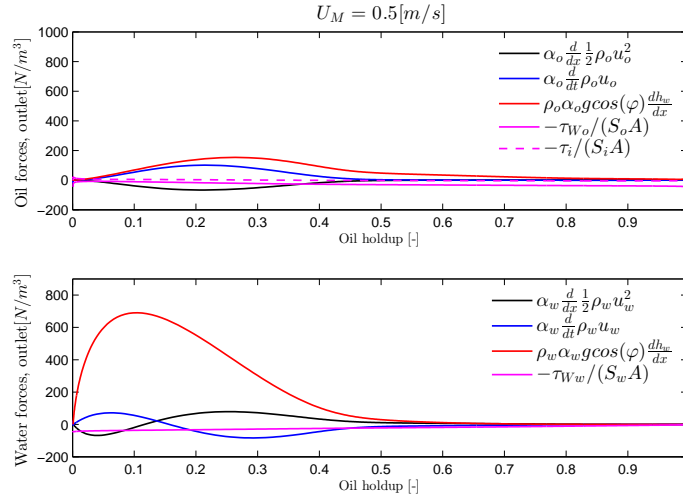


Figure 36: Oil momentum equation terms (top figure) and water (bottom figure), at $x = 16[m]$ with $U_M = 0.5$

For low mixture velocity it is obvious that the dominating term when the oil front hits the water, is the level gradient in both momentum equations, namely $\rho_o \alpha_o g \cos(\varphi) \frac{dh_w}{dx}$ and $\rho_w \alpha_w g \cos(\varphi) \frac{dh_w}{dx}$. The spatial acceleration (convective acceleration) and the temporal (local) acceleration are relatively small and they become zero after the oil front hits the water. *The shear stress on the water layer at the pipe inlet is increasing non-physically after the oil fills the pipe. This is due to the limitation of the model, where we can never have absolute zero holdup. Therefore, the remaining amount of water would be almost nothing (order of magnitude 1e-3).*

Therefore, this increasing force belongs to a non-existing water layer and should be neglected.

6.1.3 Case III: $U_M = 1$

Plotting the left hand side of the momentum equations

$$\alpha_o \frac{\partial p}{\partial x} = \dots$$

$$\alpha_w \frac{\partial p}{\partial x} = \dots$$

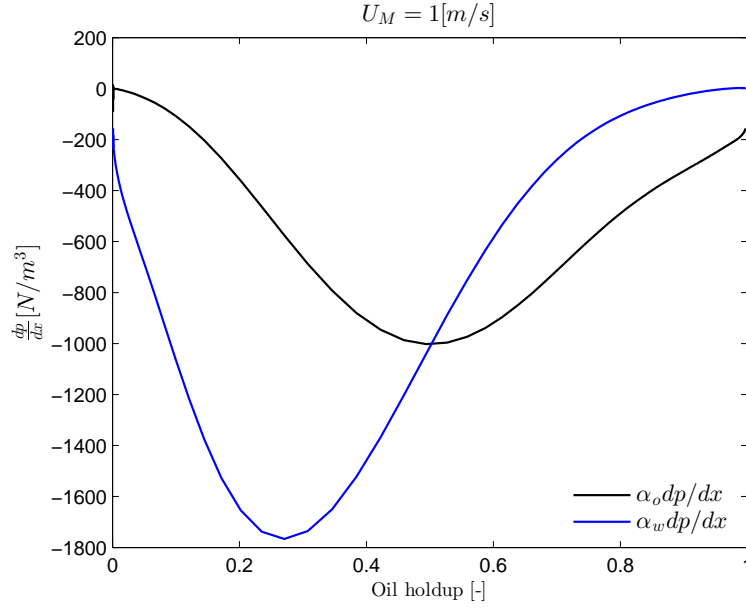


Figure 37: Pressure forces for oil and water layers, at $x = 16[m]$, $U_M =$

Plotting all the terms on the right hand side of the momentum equations

$$\dots = -\frac{\tau_{W_o} S_o}{A} - \frac{\tau_i S_i}{A} - \alpha_o \frac{\partial}{\partial t} (\rho_o u_o) + \alpha_o \frac{\partial}{\partial x} \left(\frac{1}{2} \rho_o u_o^2 \right) - \rho_o \alpha_o g \frac{\partial h_w}{\partial x} \cos \beta$$

$$\dots = -\frac{\tau_{W_w} S_w}{A} + \frac{\tau_i S_i}{A} - \alpha_w \frac{\partial}{\partial t} (\rho_w u_w) + \alpha_w \frac{\partial}{\partial x} \left(\frac{1}{2} \rho_w u_w^2 \right) - \rho_w \alpha_w g \frac{\partial h_w}{\partial x} \cos \beta$$

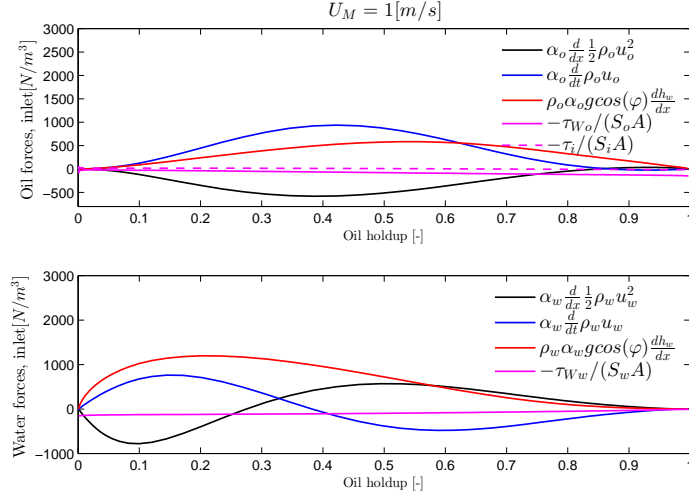


Figure 38: Oil momentum equation terms (top figure) and water (bottom figure), at $x = 1[m]$ with $U_M = 1$

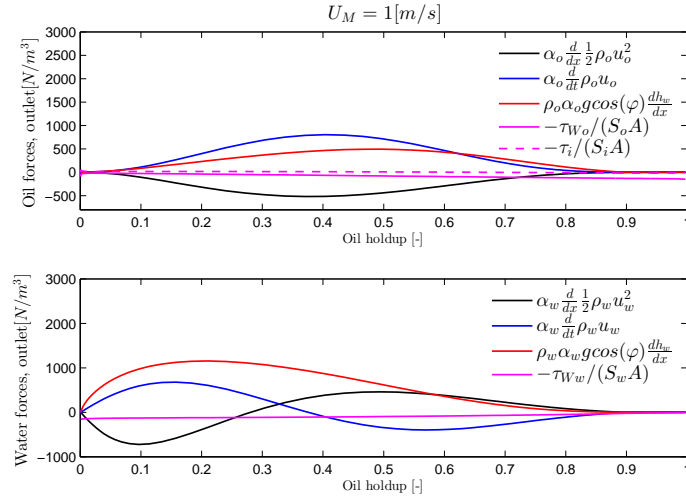


Figure 39: Oil momentum equation terms (top figure) and water (bottom figure), at $x = 16[m]$ with $U_M = 1$

As the velocity of the mixture has increased considerably, the level gradient, no longer plays an important role in the two momentum equations, however in this case the temporal and spatial derivatives dominate the solution. Later on when the pipe is almost filled with oil, it is only the shear stress that remains to balance pressure gradient in the momentum equation.

6.1.4 Case IV: $U_M = 5$

Plotting the left hand side of the momentum equations

$$\alpha_o \frac{\partial p}{\partial x} = \dots$$

$$\alpha_w \frac{\partial p}{\partial x} = \dots$$

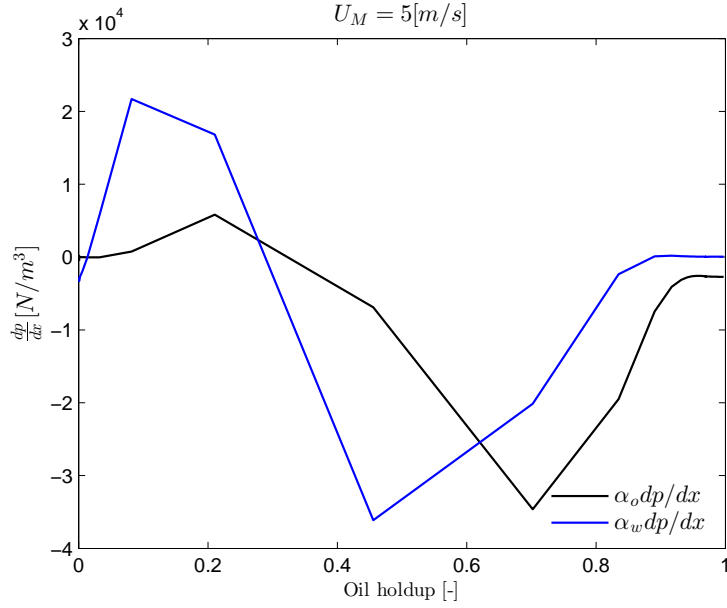


Figure 40: Pressure forces for oil and water layers, at $x = 16[m]$, $U_M = 5$

Plotting all the terms on the right hand side of the momentum equations

$$\dots = -\frac{\tau_{W_o} S_o}{A} - \frac{\tau_i S_i}{A} - \alpha_o \frac{\partial}{\partial t} (\rho_o u_o) + \alpha_o \frac{\partial}{\partial x} \left(\frac{1}{2} \rho_o u_o^2 \right) - \rho_o \alpha_o g \frac{\partial h_w}{\partial x} \cos \beta$$

$$\dots = -\frac{\tau_{W_w} S_w}{A} + \frac{\tau_i S_i}{A} - \alpha_w \frac{\partial}{\partial t} (\rho_w u_w) + \alpha_w \frac{\partial}{\partial x} \left(\frac{1}{2} \rho_w u_w^2 \right) - \rho_w \alpha_w g \frac{\partial h_w}{\partial x} \cos \beta$$

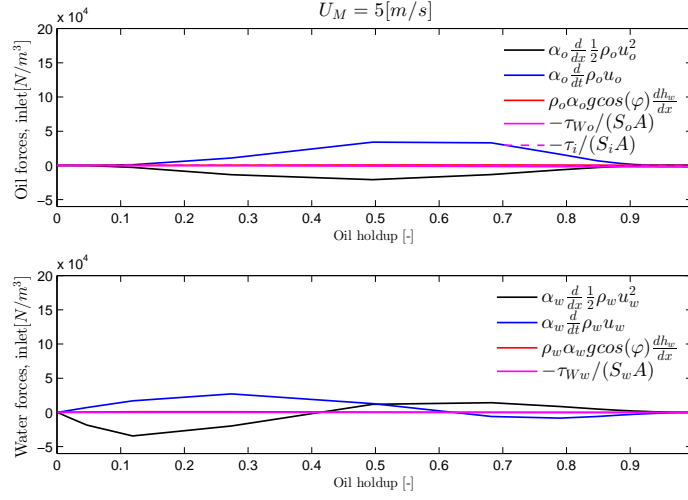


Figure 41: Oil momentum equation terms (top figure) and water (bottom figure), at $x = 1[m]$ with $U_M = 5$

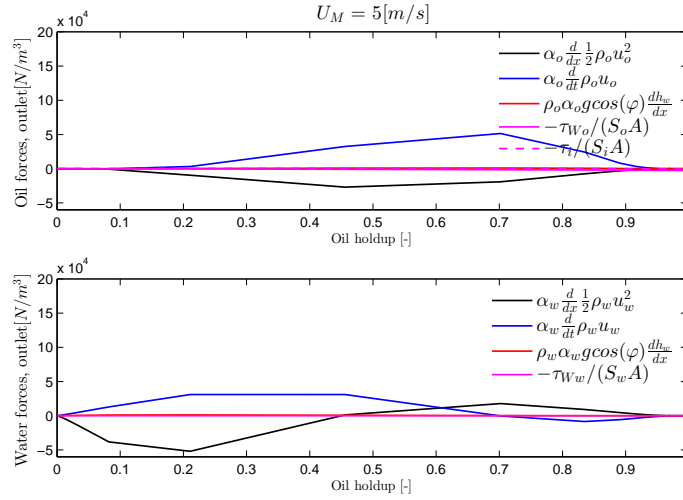


Figure 42: Oil momentum equation terms (top figure) and water (bottom figure), at $x = 16[m]$ with $U_M = 5$

With increasing the mixture velocity even more, the effect of level gradient becomes noticeably smaller than the acceleration terms. However, the acceleration terms act more or less symmetrically around the x-axis. Therefore, in effect it is still important to pay attention to the level gradient term. The resultant of all these forces will balance the pressure gradient.

7 Conclusion

Two fluid models have been developed with application for oil-water flushing. The properties of the fluids have been chosen based on Oil, Exxsol D80, $\mu_o = 1.79 [cP]$ and tapped water, $\mu_w = 1.11 [cP]$. The dynamic behavior of the models have been studied and compared with the stationary model. Regarding the dynamic models:

- Models I and II proved to be quite similar and have almost identical results according to the sensitivity analysis. Therefore, the results discussed here, apply to both models.
- For both the dynamic and stationary model, the oil front gets steeper as the mixture velocity increases.
- Considering the oil holdup diagrams, the oil front approximately the same along the pipe.
- There is a diffusion problem that needs to be addressed. The bigger the steps (dx) become, the answer (oil/water holdup curve), looks more spread out throughout the cell length that is the solution domain. The oil fronts are rather sharp where they hit the water, so if we do not choose a cell length small enough according to the grid study, the answer would look more diffused than in reality.
- The models developed in this work, have two singular points, at mathematically absolute one phase flow, either oil ($\alpha_o = 0$) or water ($\alpha_w = 0$). So transition from one-phase to two-phase flows should be implemented carefully with small time steps. The absent of a phase is modeled numerically by such a low phase fraction as $\alpha = 0.001$ or less.

Regarding the different behavior of the dynamic and the stationary models:

- The flushing cases for low velocities are dominated by the level gradient. The sensitivity analysis in chapter 5, confirms that the dynamic and stationary solutions are almost identical for low mixture velocities. therefore the acceleration terms in the dynamic model are not significant for low velocities
- For high mixture velocities, the order of magnitude of the acceleration terms, reaches the one of the level gradient. However, it seems that the acceleration terms, spatial and temporal, for most of the solution, are acting symmetrically around the x-axis, in this case they cancel each other out. This is sometimes the case, the acceleration terms might both have the same sign, and then they would make a difference in the dynamic model.
- Modeling the level gradient accurately, turns out to be very important as it seems to be the dominant term of both dynamic and stationary equations.

Recommendations

- The models developed in Matlab, work fine for laboratory scale pipes. For flow modeling for long pipelines, which require longer simulation time and bigger grid, it is recommended to move to C, which is faster.
- The time steps used can become larger by using an implicit scheme.

Appendices

A Model I Matlab code

```
%-----  
% Explicit Transient Solver for Dynamic Holdup Equation  
% Ahmadreza Rahbari 2013  
%-----  
clc;  
clear;  
global PROP;  
  
PROP=Properties(); % globals  
RHOO=PROP.RHOO;  
RHOW=PROP.RHOW;  
Pipe_angle=PROP.Angle;  
Length=PROP.Pipe_Length;  
  
%-----Boundary Conditions-----  
%If one of phase-fractions (AO or AW) is '0' use a very small number like ↔  
    '0.0001'  
%For single phase simulation => USO=0 or USW=0  
  
AO_BC=0.999; %[-]  
AW_BC=1-AO_BC; %[-]  
USO_BC=AO_BC*PROP.UM_constant; %[m3/s/m2]  
USW_BC=AW_BC*PROP.UM_constant; %[m3/s/m2]  
  
%Calculating the boundary condition variables from the data above  
[UO_BC,UW_BC,UM_BC,Beta_BC,V_BC] = Boundary_Conditions(USO_BC,USW_BC,AO_BC,AW_BC↔  
    );  
  
%-----Initial Conditions-----  
%Values at t=0 inside the cells (pipe)  
AO_init= 1.0000e-03;  
AW_init=1-AO_init;  
USO_init=AO_init*PROP.UM_constant;  
USW_init=AW_init*PROP.UM_constant;  
  
%The same function (Boundary_Conditions) is used to calculate the initial  
%values in the cells (pipe) because the calculations are identical.  
[UO_init,UW_init,UM_init,Beta_init,V_init] =...  
    Boundary_Conditions(USO_init,USW_init,AO_init,AW_init);  
%-----  
dt=PROP.delta_t; %Time step in the explicit solver  
dx=PROP.delta_x; %Length step in the explicit solver[m]  
Duration=PROP.Simulation_time; %[s] (How many seconds the simulation runs from ↔  
    t=0)  
imax=floor(Length/dx); %Calculation the dimensions of Beta and V based on time↔  
    step and pipe length  
nmax=Duration/dt;  
  
Beta=zeros(1,imax+2); %Each column has values for a certain time step from t=0↔  
    to t=nmax  
V=Beta;  
AO=Beta;  
AW=Beta;
```



```

UO=Beta;
UW=Beta;
USO=Beta;
USW=Beta;

%Imposing the boundary conditions in the first array in Beta and V
%matrices (ghost cells)
Beta(:,1)=Beta_BC;
V(:,1)=V_BC;
AO(:,1)=AO_BC;
AW(:,1)=AW_BC;
USO(:,1)=USO_BC;
USW(:,1)=USW_BC;
%added recently
UO(:,1)=USO_BC/AO_BC;
UW(:,1)=USW_BC/AW_BC;
UM=UM_BC;

%Imposing the initial conditions in the first row of the Beta and V
%matrices (at t=0, n=1)
Beta(1,2:imax+1)=Beta_init;
V(1,2:imax+1)=V_init;
AO(1,2:imax+1)=AO_init;
AW(1,2:imax+1)=AW_init;
USO(1,2:imax+1)=USO_init;
USW(1,2:imax+1)=USW_init;
%added recently
UO(1,2:imax+1)=USO_init/AO_init;
UW(1,2:imax+1)=USW_init/AW_init;

Beta_new=Beta;
V_new=V;

dt_interval=0.01; %capturing the results every 0.01 [s]
NumberOfPoints=Duration/dt_interval;
AO_result=zeros(NumberOfPoints+1,imax);
AW_result=zeros(NumberOfPoints+1,imax);
USO_result=zeros(NumberOfPoints+1,imax);
USW_result=zeros(NumberOfPoints+1,imax);
Beta_result=zeros(NumberOfPoints+1,imax);
V_result=zeros(NumberOfPoints+1,imax);
time_result=zeros(NumberOfPoints+1,1);

AO_result(:,1)=AO_BC; % First array in every row= Boundary Condition= constant↔
, does not change with time
AW_result(:,1)=AW_BC;
USO_result(:,1)=USO_BC;
USW_result(:,1)=USW_BC;
Beta_result(:,1)=Beta_BC;
V_result(:,1)=V_BC;
time_result(1,1)=0;

AO_result(1,2:imax+1)=AO_init;
AW_result(1,2:imax+1)=AW_init;
USO_result(1,2:imax+1)=USO_init;
USW_result(1,2:imax+1)=USW_init;
Beta_result(1,2:imax+1)=Beta_init;
V_result(1,2:imax+1)=V_init;

j=2;
z=1;
m=0; %The beginning of the time! t=0

```

```

TimeRatio=floor(dt_interval/dt); %ratio of time steps for recording the data ↔
to the solver's time steps, this determines how many n's should count before↔
we record the data.

for n=1:nmax %Time loop counter
    m=m+dt; %counts real time passing [s]

    if rem(n/TimeRatio,1) == 0

        z=z+1;
        for j=2:imax+1
            AO_result(z,j)=AO(1,j);
            AW_result(z,j)=AW(1,j);
            USO_result(z,j)=UO(1,j)*AO(1,j);
            USW_result(z,j)=UW(1,j)*AW(1,j);
            Beta_result(z,j)=Beta(1,j);
            V_result(z,j)=V(1,j);
            time_result(z,1)=(z-1)*dt_interval;

        end

    end

    Beta=Beta_new;
    V=V_new;

    for j=2:imax+1
        %Updating Beta and V for the new time step
        %calculating the frictions based on hold up and velocity (the
        %source term in the slip momentum equation)
        AO(1,j)=(Beta(1,j)-RHOO)/(RHOW-RHOO);
        AW(1,j)=(Beta(1,j)-RHOW)/(RHOO-RHOW);
        UO(1,j)=(V(1,j)/Beta(j)).*((Beta(1,j)-RHOW)/(RHOO-RHOW))+UM;
        UW(1,j)=-(V(1,j)/Beta(1,j)).*((Beta(1,j)-RHOO)/(RHOW-RHOO))+UM;
        [FO,FW,FI]=FrictionTerms(UO(1,j),UW(1,j),AO(1,j),AW(1,j),RHOO,RHOW);
        USO(1,j)=AO(1,j).*UO(1,j);
        USW(1,j)=AW(1,j).*UW(1,j);

        C1=RHOO-RHOW;
        qv=-(FO/(AO(1,j)))+(FW/(AW(1,j)))-(FI/((AO(1,j))*AW(1,j)))-(C1)*9.81*↔
            sin(Pipe_angle);

        if any(~isreal(FO))
            stop
        end

        Theta_3=WettedAngle(AO(1,j+1));
        Theta_2=WettedAngle(AO(1,j));
        Theta_1=WettedAngle(AO(1,j-1));
        h_3=0.5*PROP.Diam*(1-cos(Theta_3));
        h_2=0.5*PROP.Diam*(1-cos(Theta_2));
        h_1=0.5*PROP.Diam*(1-cos(Theta_1));

        if j==imax+1
            Beta(1,j+1)=2*Beta(1,j)-Beta(1,j-1);
            V(1,j+1)=2*V(1,j)-V(1,j-1);
            h_3=2*h_2-h_1;
        end

        Beta_right=0.5*(Beta(1,j)+Beta(1,j+1));
    end
end

```

```

Beta_left=0.5*(Beta(1,j-1)+Beta(1,j));

h_right_boundary=0.5*(h_2+h_3);
h_left_boundary=0.5*(h_1+h_2);

Mass_Flux_out=((V(1,j))./(Beta_right)).*(((Beta_right-RH00).*(←
Beta_right-RHOW))./(C1)))+UM.*Beta(1,j);
Mass_Flux_in=((V(1,j-1))./(Beta_left)).*(((Beta_left-RH00).*(Beta_left-←
RHOW))./(C1)))+UM.*Beta(1,j-1);

CC=1/(2*(RH00-RHOW));

Momentum_Flux_out=CC*(((V(1,j)))^2-((V(1,j)^2)*RH00*RHOW)/((Beta_right)←
^2))+UM*(V(1,j))+(C1)*9.81*cos(Pipe_angle)*h_right_boundary;
Momentum_Flux_in=CC*(((V(1,j-1)))^2-((V(1,j-1)^2)*RH00*RHOW)/((Beta_left)←
^2))+UM*(V(1,j-1))+(C1)*9.81*cos(Pipe_angle)*h_left_boundary;

Beta_new(1,j)=(Beta(1,j)+(dt/dx)*(Mass_Flux_in-Mass_Flux_out));
V_new(1,j)=V(1,j)+dt*((Momentum_Flux_in-Momentum_Flux_out)/dx+qv);

end
end

```

B Model II Matlab code

```
%-----  
% Explicit Transient Solver for Dynamic Holdup Equation  
% Ahmadreza Rahbari 2013  
%-----  
clc;  
clear;  
global PROP;  
  
PROP=Properties(); % globals  
RHO0=PROP.RHO0;  
RHOW=PROP.RHOW;  
Pipe_angle=PROP.Angle;  
Length=PROP.Pipe_Length;  
  
%-----Boundary Conditions-----  
%If one of phase-fractions (AO or AW) is '0' use a very small number like ↔  
'0.0001'  
%For single phase simulation => USO=0 or USW=0  
  
AO_BC=0.999; %[-]  
AW_BC=1-AO_BC; %[-]  
USO_BC=AO_BC*PROP.UM_constant; %[m3/s/m2]  
USW_BC=AW_BC*PROP.UM_constant; %[m3/s/m2]  
  
%Calculating the boundary condition variables from the data above  
[UO_BC,UW_BC,UM_BC,RHOM_BC,Us_BC] = Boundary_Conditions(USO_BC,USW_BC,AO_BC,↔  
AW_BC);  
  
%-----Initial Conditions-----  
%Values at t=0 inside the cells (pipe)  
AO_init= 1.0000e-03;  
AW_init=1-AO_init;  
USO_init=AO_init*PROP.UM_constant;  
USW_init=AW_init*PROP.UM_constant;  
  
%The same function (Boundary_Conditions) is used to calculate the initial  
%values in the cells (pipe) because the calculations are identical.  
[UO_init,UW_init,UM_init,RHOM_init,Us_init] =...  
Boundary_Conditions(USO_init,USW_init,AO_init,AW_init);  
%-----  
dt=PROP.delta_t; %Time step in the explicit solver  
dx=PROP.delta_x; %Length step in the explicit solver[m]  
Duration=PROP.Simulation_time; %[s] (How many seconds the simulation runs from ↔  
t=0)  
imax=floor(Length/dx); %Calculation the dimensions of Beta and V based on time↔  
step and pipe length  
nmax=Duration/dt;  
  
RHOM=zeros(1,imax+2); %Each column has values for a certain time step from t=0↔  
to t=nmax  
Us=RHOM;  
AO=RHOM;  
AW=RHOM;  
UO=RHOM;  
UW=RHOM;  
USO=RHOM;
```

```

USW=RHOM;

%Imposing the boundary conditions in the first array in Beta and V
%matrices (ghost cells)
RHOM(:,1)=RHOM_BC;
Us(:,1)=Us_BC;
AO(:,1)=AO_BC;
AW(:,1)=AW_BC;
USO(:,1)=USO_BC;
USW(:,1)=USW_BC;
%added recently
UO(:,1)=USO_BC/AO_BC;
UW(:,1)=USW_BC/AW_BC;
UM=UM_BC;

%Imposing the initial conditions in the first row of the Beta and V
%matrices (at t=0, n=1)
RHOM(1,2:imax+1)=RHOM_init;
Us(1,2:imax+1)=Us_init;
AO(1,2:imax+1)=AO_init;
AW(1,2:imax+1)=AW_init;
USO(1,2:imax+1)=USO_init;
USW(1,2:imax+1)=USW_init;
%added recently
UO(1,2:imax+1)=USO_init/AO_init;
UW(1,2:imax+1)=USW_init/AW_init;

% Creating the matrices used for extracting the results and generating
% figures.
RHOM_new=RHOM;
Us_new=Us;

dt_interval=0.01; %capturing the results every 0.01 [s]
NumberOfPoints=Duration/dt_interval;
AO_result=zeros(NumberOfPoints+1,imax); %'+1' meaning including point t=0 ←
    until t=Duration with intervals of length=dt_result
AW_result=zeros(NumberOfPoints+1,imax);
USO_result=zeros(NumberOfPoints+1,imax);
USW_result=zeros(NumberOfPoints+1,imax);
RHOM_result=zeros(NumberOfPoints+1,imax);
Us_result=zeros(NumberOfPoints+1,imax);
time_result=zeros(NumberOfPoints+1,1);

AO_result(:,1)=AO_BC; % First array in every row= Boundary Condition= constant↔
    , does not change with time
AW_result(:,1)=AW_BC;
USO_result(:,1)=USO_BC;
USW_result(:,1)=USW_BC;
RHOM_result(:,1)=RHOM_BC;
Us_result(:,1)=Us_BC;
time_result(1,1)=0;

AO_result(1,2:imax+1)=AO_init;
AW_result(1,2:imax+1)=AW_init;
USO_result(1,2:imax+1)=USO_init;
USW_result(1,2:imax+1)=USW_init;
RHOM_result(1,2:imax+1)=RHOM_init;
Us_result(1,2:imax+1)=Us_init;

j=2;
z=1;

```

```

m=0;    %The beginning of the time! t=0

TimeRatio=floor(dt_interval/dt);    %ratio of time steps for recording the data ↔
    to the solver's time steps, this determines how many n's should count before↔
    we record the data.

for n=1:nmax    %Time loop counter
    m=m+dt;    %counts real time passing [s]

    if rem(n/TimeRatio,1) == 0

        z=z+1;
        for j=2:imax+1
            AO_result(z,j)=AO(1,j);
            AW_result(z,j)=AW(1,j);
            USO_result(z,j)=UO(1,j)*AO(1,j);
            USW_result(z,j)=UW(1,j)*AW(1,j);
            RHOM_result(z,j)=RHOM(1,j);
            Us_result(z,j)=Us(1,j);
            time_result(z,1)=(z-1)*dt_interval;
        end
    end

    RHOM=RHOM_new;
    Us=Us_new;
    for j=2:imax+1
        %Updating Beta and V for the new time step
        %calculating the frictions based on hold up and velocity (the
        %source term in the slip momentum equation)
        AO(1,j)=(RHOM-RHOM(1,j))./(RHOW-RHOO);
        AW(1,j)=(RHOM(1,j)-RHOO)./(RHOW-RHOO);
        UO(1,j)=UM+AW(1,j).*Us(1,j);
        UW(1,j)=UM-AO(1,j).*Us(1,j);
        [FO,FW,FI]=FrictionTerms(UO(1,j),UW(1,j),AO(1,j),AW(1,j),RHOO,RHOW);
        if any(~isreal(FO))
            stop
        end
        USW(1,j)=AW(1,j).*UW(1,j);
        USO(1,j)=AO(1,j)*UO(1,j);

        C1=RHOW-RHOO;
        qv=(FO/(AO(1,j)))-(FW/(AW(1,j)))+(FI/((AO(1,j))*AW(1,j)))-(C1)*9.81*←
            sin(Pipe_angle);

        Theta_3=WettedAngle(AO(1,j+1));
        Theta_2=WettedAngle(AO(1,j));
        Theta_1=WettedAngle(AO(1,j-1));
        h_3=0.5*PROP.Diam*(1-cos(Theta_3));
        h_2=0.5*PROP.Diam*(1-cos(Theta_2));
        h_1=0.5*PROP.Diam*(1-cos(Theta_1));

        if j==imax+1
            RHOM(1,j+1)=2.*RHOM(1,j)-RHOM(1,j-1);
            Us(1,j+1)=2.*Us(1,j)-Us(1,j-1);
            h_3=2*h_2-h_1;
        end
        RHOM_right=0.5*(RHOM(1,j)+RHOM(1,j+1));
        RHOM_left=0.5*(RHOM(1,j)+RHOM(1,j-1));
        Us_right=0.5*(Us(1,j)+Us(1,j+1));
        Us_left=0.5*(Us(1,j)+Us(1,j-1));
        h_right_boundary=0.5*(h_2+h_3);
    end
end

```

```

h_left_boundary=0.5*(h_1+h_2);

AO_right=(RHOW-RHOM_right)/C1;
AW_right=(RHOM_right-RHOO)/C1;

AO_left=(RHOW-RHOM_left)/C1;
AW_left=(RHOM_left-RHOO)/C1;

Mass_Flux_out=RHOM(1,j)*UM-(C1)*AO_right*AW_right.*Us(1,j);
Mass_Flux_in=RHOM(1,j-1)*UM-(C1)*AO_left*AW_left.*Us(1,j-1);

RHOM_new(1,j)=RHOM(1,j)+(dt/dx)*(Mass_Flux_in-Mass_Flux_out);

Momentum_Flux_out=0.5*(RHOW*(AO_right).^2-RHOO*(AW_right).^2).*(Us(1,j)↔
.^2)-(RHOW*AO_right+RHOO*AW_right).*(UM.*Us(1,j))+(C1).*9.81.*cos(↔
Pipe_angle).*(h_right_boundary);
Momentum_Flux_in=0.5*(RHOW*(AO_left).^2-RHOO*(AW_left).^2).*(Us(1,j-1)↔
.^2)-(RHOW*AO_left+RHOO*AW_left).*(UM.*Us(1,j-1))+(C1).*9.81.*cos(↔
Pipe_angle).*(h_left_boundary);

Us_new(1,j)=(1./(RHOM_new(1,j)-RHOW-RHOO)).*(((RHOM(1,j)-RHOO-RHOW).*Us↔
(1,j)+dt*(((Momentum_Flux_in-Momentum_Flux_out)./dx)+qv));

end
end

```

C Closure models, friction Matlab code

```
function [FO,FW,FI]=FrictionTerms(UO,UW,AO,AW,RHOO,RHOW)

global PROP;

Ur=UO-UW;
%-----Angel-----
theta=WettedAngle(AO);
%-----Geometry-----
SW=theta*PROP.Diam;
SO=pi*PROP.Diam-SW;
SI=PROP.Diam*sin(theta);
%-----Reynold-----
%Water: open channel flow, Oil: closed channel flow
Dho=4*AO.*PROP.Area./(SO+SI);
Dhw=4*AW.*PROP.Area./(SW+1e-100);
Reo=Reynold(Dho,abs(UO),RHOO,PROP.muo);
Rew=Reynold(Dhw,abs(UW),RHOW,PROP.muw);
%-----Friction factor (Turbulent and Laminar)-----
foTur=Haaland(Reo,Dho+1e-1000);
fwTur=Haaland(Rew,Dhw+1e-1000);
foLam=64/Reo;
fwLam=64/Rew;

if Reo<300
    fo=foLam;
else
    fo = max([foLam,foTur]);
end

if Rew<300
    fw=fwLam;
else
    fw = max([fwLam,fwTur]);
end

fi=fo; %Friction at the interface is taken equal to the oil layer friction

%-----Friction terms-----
t1=8*PROP.Area;
FO=RHOO.*fo.*abs(UO).*UO.*SO/t1;
FW=RHOW.*fw.*abs(UW).*UW.*SW/t1;
FI=RHOO.*fi.*abs(Ur).*Ur.*SI/t1;
```


References

- [1] Lene Amundsen. *An experimental study of oil-water flow in horizontal and inclined pipes*. PhD thesis, Norwegian University of Science and Technology, Department of Energy and Process Engineering, 2011.
- [2] S Arirachakaran, KD Oglesby, MS Malinowsky, O Shoham, JP Brill, et al. An analysis of oil/water flow phenomena in horizontal pipes. In *SPE Production Operations Symposium*. Society of Petroleum Engineers, 1989.
- [3] Kjell H Bendiksen, Dag Maines, Randi Moe, Sven Nuland, et al. The dynamic two-fluid model olga: Theory and application. *SPE production engineering*, 6(02):171–180, 1991.
- [4] M Bonizzi and RI Issa. On the simulation of three-phase slug flow in nearly horizontal pipes using the multi-fluid model. *International journal of multiphase flow*, 29(11):1719–1747, 2003.
- [5] Ove Bratland. Pipe flow 2. *Multi-Phase Flow Assurance*, 2010.
- [6] Clayton T Crowe. *Multiphase flow handbook*. CRC Press, 2005.
- [7] Thomas J Danielson, Kris M Bansal, Ronny Hansen, Emile Leporcher, et al. Leda: the next multiphase flow performance simulator. In *12th International Conference on Multiphase Production Technology*. BHR Group, 2005.
- [8] Xiaoju Du. *Numerical Solvers for Transient Two-Phase Flow*. PhD thesis, Norwegian University of Science and Technology, Department of Energy and Process Engineering, 2013.
- [9] S. Guet, O.M.H. Rodriguez, R.V.A. Oliemans, and N. Brauner. An inverse dispersed multiphase flow model for liquid production rate determination. *International Journal of Multiphase Flow*, 32(5):553 – 567, 2006.
- [10] T.K. Kjeldby and O.J. Nydal. A lagrangian three-phase slug tracking framework. *International Journal of Multiphase Flow*, 56(0):184 – 194, 2013.
- [11] Tor Kindsbekken Kjeldby. *Lagrangian Three-phase Slug Tracking Methods*. PhD thesis, Norwegian University of Science and Technology, Department of Energy and Process Engineering, 2013.
- [12] W. Amaranath Sena Kumara. *An Experimental Study of Oil-Water Flow in Pipes*. PhD thesis, Norwegian University of Science and Technology, Faculty of Engineering Science and Technology, 2011.
- [13] OJ Nydal and S Banerjee. Dynamic slug tracking simulations for gas-liquid flow in pipelines. *Chemical Engineering Communications*, 141(1):13–39, 1996.
- [14] CL Pauchon, Hasmuekh Dhulesia, et al. Tacite: A transient tool for multiphase pipeline and well simulation. In *SPE Annual Technical Conference and Exhibition*. Society of Petroleum Engineers, 1994.
- [15] Trygve Wangensteen. *Mixture-Slip Flux Splitting for Numerical Computation of 1-D Two-Phase Flow*. PhD thesis, Norwegian University of Science and Technology, Department of Energy and Process Engineering, 2010.